

FINAL  
CONTRACT REPORT

**EXPERIMENTAL  
AND ANALYTICAL INVESTIGATIONS  
OF PILES AND ABUTMENTS  
OF INTEGRAL BRIDGES**

SAMI ARSOY, Ph.D.  
RICHARD M. BARKER, Ph.D., P.E.  
and  
J. MICHAEL DUNCAN, Ph.D., P.E.

The Charles E. Via, Jr.  
Department of Civil and Environmental Engineering  
Virginia Polytechnic Institute and State University

Contract Research Sponsored by  
Virginia Transportation Research Council



**Standard Title Page - Report on Federally Funded Project**

1. Report No. FHWA/VTRC 02-CR6	2. Government Accession No.	3. Recipient's Catalog No.	
4. Title and Subtitle Experimental and Analytical Investigations of Piles and Abutments of Integral Bridges		5. Report Date March 2002	
		6. Performing Organization Code	
7. Author(s) Sami Arsoy, Richard M. Barker, and J. Michael Duncan		8. Performing Organization Report No. VTRC 02-CR6	
9. Performing Organization and Address  Virginia Transportation Research Council 530 Edgemont Road Charlottesville, VA 22903		10. Work Unit No. (TRAIS)	
		11. Contract or Grant No. 99-2114-05	
12. Sponsoring Agencies' Name and Address  Virginia Department of Transportation      FHWA 1401 E. Broad Street                              P.O. Box 10249 Richmond, VA 23219                                Richmond, VA 23240		13. Type of Report and Period Covered Final July 1999 – September 2001	
		14. Sponsoring Agency Code	
15. Supplementary Notes			
<p>16. Abstract</p> <p>This research investigated, through experimental and analytical studies, the complex interactions that take place between the structural components of an integral bridge and the adjoining soil. The ability of piles and abutments to withstand thermally induced cyclic loads was investigated by conducting large-scale cyclic load tests. Three pile types and three integral abutments with hinges were tested in the laboratory. Experiments simulated 75 years of bridge life. Numerical analyses were conducted to analyze the interactions among the abutment, the approach fill, the foundation soil, and the foundation piles.</p> <p>The results indicated that H-piles are most suitable for supporting integral abutments. Concrete piles and pipe piles were too stiff in response to repeated lateral loads, resulting in tension cracks at the connection with the abutment. Further, a hinge in the integral abutment effectively reduces pile stresses by absorbing some of the rotational movement.</p>			
17 Key Words integral bridge, cyclic loading, thermal induction		18. Distribution Statement No restrictions. This document is available to the public through NTIS, Springfield, VA 22161.	
19. Security Classif. (of this report) Unclassified	20. Security Classif. (of this page) Unclassified	21. No. of Pages 55	22. Price

**FINAL CONTRACT REPORT**

**EXPERIMENTAL AND ANALYTICAL INVESTIGATIONS  
OF THE PILES AND ABUTMENTS OF INTEGRAL BRIDGES**

**Sami Arsoy, Ph.D., Richard M. Barker Ph.D., P.E., and J. Michael Duncan Ph.D., P.E.  
The Charles E. Via, Jr., Department of Civil and Environmental Engineering  
Virginia Polytechnic Institute and State University**

*Project Monitor*

Edward J. Hoppe, Virginia Transportation Research Council

Contract Research Sponsored by  
Virginia Transportation Research Council

Virginia Transportation Research Council  
(A Cooperative Organization Sponsored Jointly by the  
Virginia Department of Transportation and  
the University of Virginia)

Charlottesville, Virginia

March 2002  
VTRC 02-CR6

## **NOTICE**

The project that is the subject of this report was done under contract for the Virginia Department of Transportation, Virginia Transportation Research Council. The contents of this report reflect the views of the authors, who are responsible for the facts and the accuracy of the data presented herein. The contents do not necessarily reflect the official views or policies of the Virginia Department of Transportation, the Commonwealth Transportation Board, or the Federal Highway Administration. This report does not constitute a standard, specification, or regulation.

Each contract report is peer reviewed and accepted for publication by Research Council staff with expertise in related technical areas. Final editing and proofreading of the report are performed by the contractor.

Copyright 2002 by the Virginia Department of Transportation.

## ABSTRACT

This research project investigated, through experimental and analytical studies, the complex interactions that take place between the structural components of an integral bridge and the soil. The ability of piles and abutments to withstand cyclic loads was investigated by conducting large-scale cyclic load tests. Three pile types and three integral abutments with hinges were tested in the laboratory. Experiments simulated 75 years of bridge life by applying more than 27,000 displacement cycles to each specimen. Numerical analyses were conducted to investigate the interactions among the abutment, the approach fill, the foundation soil, and the piles.

The original VDOT integral abutment with a hinge underwent shear key failure as observed in two large-scale laboratory tests. The revised hinge detail was not damaged. Both abutments tolerated 75 years worth of displacement cycles without any appreciable change in behavior. Integral abutments with hinges are recommended for longer integral bridges because they can reduce pile stresses. As the need to build longer integral bridges grows, the role of integral abutments with hinges is expected to become more important.

The data from the experimental program indicate that weak-axis steel H-piles are the best pile type for support of integral abutment bridges. The concrete pile tested was too stiff and is not recommended because under repeated lateral loads, tension cracks developed in the pile at the connection to the abutment. The pipe pile tested also had high flexural stiffness, which resulted in the development of a large shear force that could not be transferred to the abutment. For these reasons, stiff concrete and pipe piles are not recommended for support of integral bridges.

Numerical analyses indicated that the interactions between the approach fill and the foundation soils create favorable conditions for stresses in piles supporting integral bridges. Because of these interactions, the foundation soil acts as if it were softer, resulting in a reduction in pile stresses compared to a single pile in the same soil without the approach fill above it.

# FINAL CONTRACT REPORT

## EXPERIMENTAL AND ANALYTICAL INVESTIGATIONS OF THE PILES AND ABUTMENTS OF INTEGRAL BRIDGES

**Sami Arsoy, Ph.D., J. Michael Duncan Ph.D., P.E., and Richard M. Barker Ph.D., P.E.**  
**Virginia Polytechnic Institute and State University**

### INTRODUCTION

The term *integral bridge* usually refers to jointless bridges with short stub-type abutments connected rigidly to the bridge deck without joints. This rigid connection allows the abutment and the superstructure to act as a single structural unit (Figure 1). Typically, single rows of piles provide foundation support for the abutments.

Eliminating joints from bridges creates concerns about the piles and abutments of integral bridges because they are subjected to temperature-induced cyclic lateral displacements. As temperatures change daily and seasonally, the length of integral bridges increases and decreases, pushing the abutment against the approach fill and pulling it away. As a result, the bridge superstructure, the abutment, the approach fill, the foundation piles, and the foundation soil are all subjected to cyclic loading. Understanding their interactions is important for effective design and satisfactory performance of integral bridges.

In addition, the ability of piles to accommodate lateral displacements is a significant factor in determining the maximum possible length of integral bridges. In order to build longer integral bridges, pile stresses should be kept low.

### PURPOSE AND SCOPE

The purpose of this research was to:

- establish the current state of knowledge with regard to cyclic loading damage to piles of integral bridges
- investigate the ability of an integral abutment with hinge to withstand cyclic loading induced by temperature variations through large-scale laboratory experiments
- investigate the ability of three pile types (H-pile, pipe pile, and prestressed reinforced concrete pile) to withstand cyclic lateral displacements induced by temperature variations
- investigate the significance of the interactions among the abutment, the approach fill, the foundation soil, and the piles through finite element analyses
- investigate the possibility of using simple procedures for designing piles supporting integral bridges.

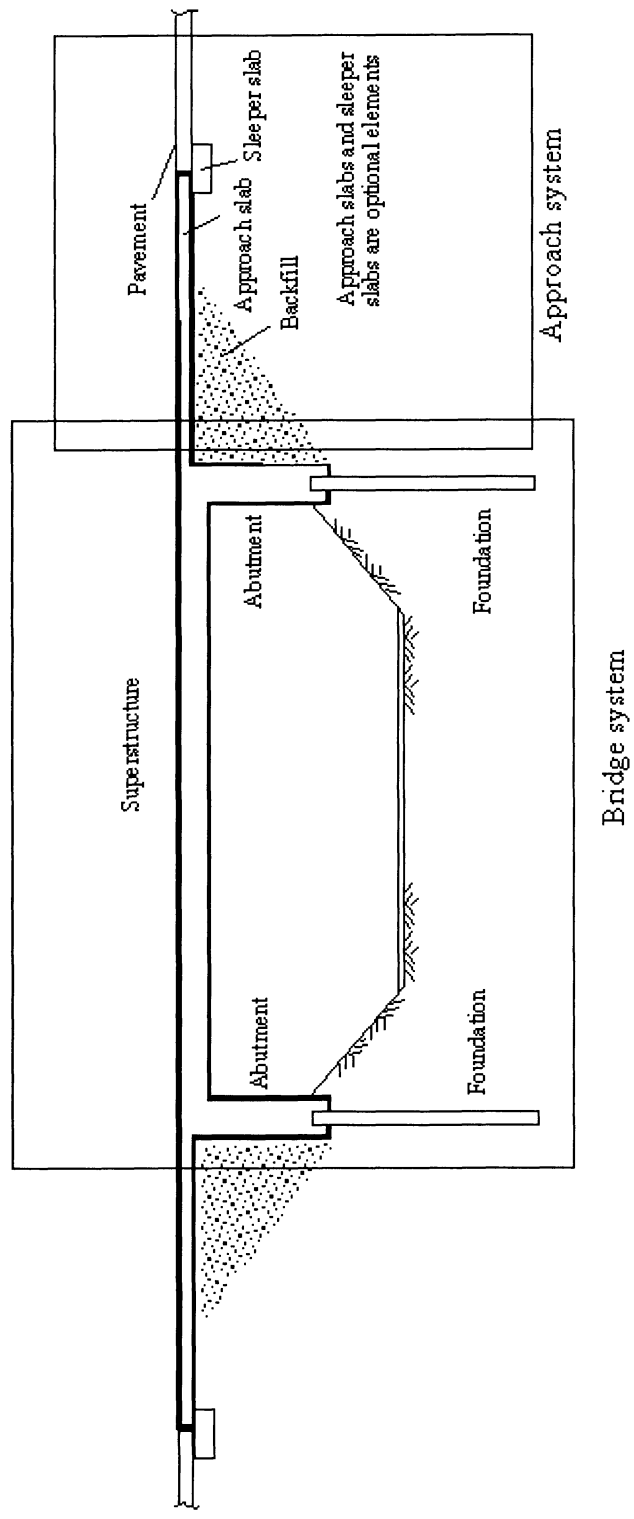


Figure 1. Simplified geometry of an integral bridge

A literature review was conducted to establish the state of knowledge with regard to cyclic loading damage to piles supporting integral abutment bridges. No cases of instrumented pipe piles or prestressed pile foundations were found. Only five studies were found that describe the performance of steel H-piles of full integral abutment bridges. These studies were concerned with the behavior of the following bridges:

- The Cass County Bridge, North Dakota
- The Boone River Bridge, Iowa
- The Maple River Bridge, Iowa
- A bridge in Rochester, Minnesota.

The Cass County Bridge is located 2 miles north of Fargo, North Dakota. The bridge is 450 ft long and 32 ft wide with no skew (Jorgenson, 1983). The bridge consists of six spans, 75 ft each, and has a concrete deck and prestressed concrete girders. The bridge is supported by HP10x42 piles oriented in weak-axis bending under abutments and strong axis bending under integral piers. The foundation piles were installed in 20-ft predrilled boreholes.

The Boone River Bridge is located in central Iowa. Girton et al. (1991) include some of the most complete and valuable data related to the performance of integral bridges. The bridge is 324.5 ft long and 40 ft wide with a skew of 45 degrees. The bridge has four continuous spans and consists of a concrete deck and prestressed concrete girders. Two of the piers of the bridge are located about 50 ft from each abutment. The third pier is located at the center of the bridge. Foundation piles are HP10x42 oriented in weak axis bending and battered 4:1 in the movement direction of the bridge. Piles were installed in 9-ft predrilled boreholes.

The Maple River Bridge is located in northwest Iowa. Girton et al. (1991) include valuable data related to the performance of integral bridges such as the Boone River Bridge. The bridge is 320 ft long and 32 ft wide with a skew of 30 degrees. The bridge has three spans and consists of a composite concrete deck and steel girders. Two piers of the bridge are located about 100 ft from each abutment. Foundation piles are HP10x42 oriented in weak axis bending and battered 3:1 in the movement direction of the bridge. Piles were installed in 12-ft predrilled boreholes.

The bridge located in Rochester, Minnesota was built in 1996 and monitored from September 1996 to September 1998. The bridge has three equal spans of 22 m each for a total length of 66 m (216 ft) and a width of 12 m (39 ft). MN/DOT Type 45M prestressed concrete bridge girders with a spacing of 3.4 m (11 ft) were used. The integral abutments were 0.9 m (3 ft) wide and 1.5 m (5 ft) high and supported by HP12x53 piles oriented in weak axis bending.

Table 1 summarizes the behavior of piles for each bridge during their monitoring period. Each bridge was monitored for approximately 2 years. During the monitoring period, bridges were subject to real-life loading, including the temperature-induced cyclic loading. Observed movements were proportional to the length of the bridges. All bridges were supported by steel H-piles. The piles were able to tolerate the loads, including those induced by temperature

variations. No sign of damage to piles was reported. It appears that steel H-piles supporting integral bridges can withstand cyclic loading as long as the maximum stresses remain equal to or less than the nominal yield stress of the pile material.

Table 1. Summary of behavior of piles supporting full integral abutment bridges

Bridge	Reference	Maximum pile stress (% of nominal yield)	Remarks
The Cass County Bridge	Jorgenson (1983)	100	Strain gages failed. Author estimated stresses based on analytical methods and concluded that maximum pile stresses were around the yield stress, and that plastic hinge formation in piles was not possible. Piles were able to tolerate 2 inches of bridge contraction and about 3 inches of total displacement without damage.
The Boone River Bridge	Girton et al. (1991)	60+	Piles were able to tolerate 1.2 inches of bridge contraction and about 2 inches of total displacement without damage.
The Maple River Bridge		75+	Piles were able to tolerate 1.6 inches of bridge contraction and about 2.5 inches of total displacement without damage.
Rochester, Minnesota Bridge	Lawver et al. (2000)	100	Piles were able to tolerate 0.65 inches of bridge contraction and 1.06 inches of total displacement without damage.

## METHODS

### Experiments on Abutments

#### Design and Construction

Standard design plans of the Virginia Department of Transportation (VDOT) were used to establish the size of the specimens. VDOT's Staunton District provided the information necessary for design and reviewed the plans before construction. The specimens were constructed and tested in the structures laboratory of Virginia Tech. Dimensions of the specimens were selected to take full advantage of the layout of the reaction floor in the lab. Arsoy (2000) documents the details of this experimental study.

Two specimens with the original detail as illustrated in Figure 2 were constructed. The construction took place between November 1999 and January 2000. The pile cap block and the abutment block of the first specimen (Specimen A) were cast on November 23, 1999, and December 8, 1999, respectively. Similarly, the pile cap block and the abutment block of the second specimen (Specimen B) were cast on November 29, 1999, and January 5, 2000, respectively. Figure 3 presents photographs from the construction.

During static load tests of the first two specimens, a deficiency in the design was discovered. Upon consultation with the Staunton District, they, as illustrated in Figure 4, developed a revised detail. The construction of the revised detail was completed in May 2000.

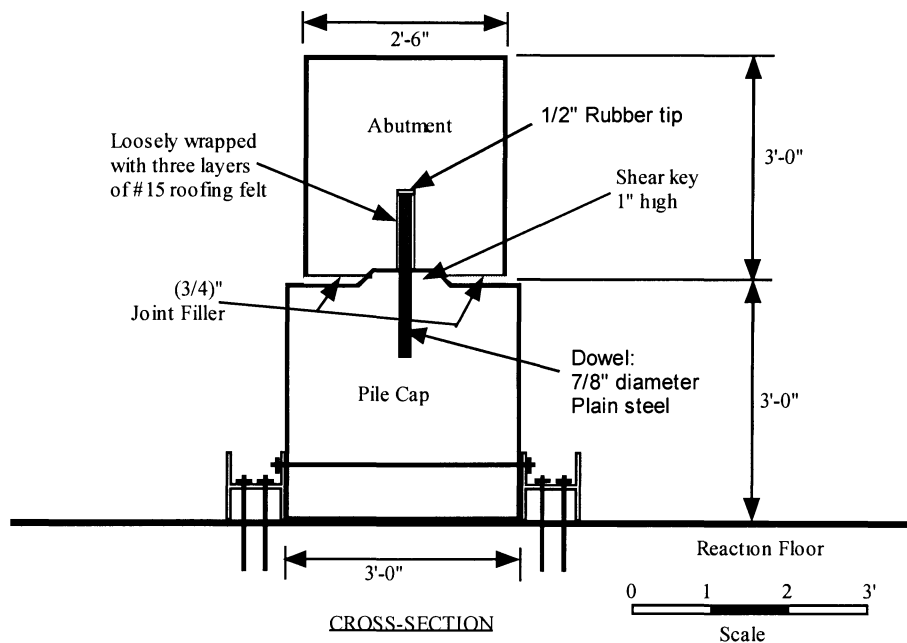


Figure 2. Schematic illustration of the initial VDOT integral abutment with hinge

The pile cap block of Specimen B was re-used. After the abutment of Specimen B was removed, the surface of the pile cap was leveled and cleaned. The revised detail was built on the surface of this recycled pile cap. Figure 5 presents a photograph from the construction of the revised detail (Specimen C).

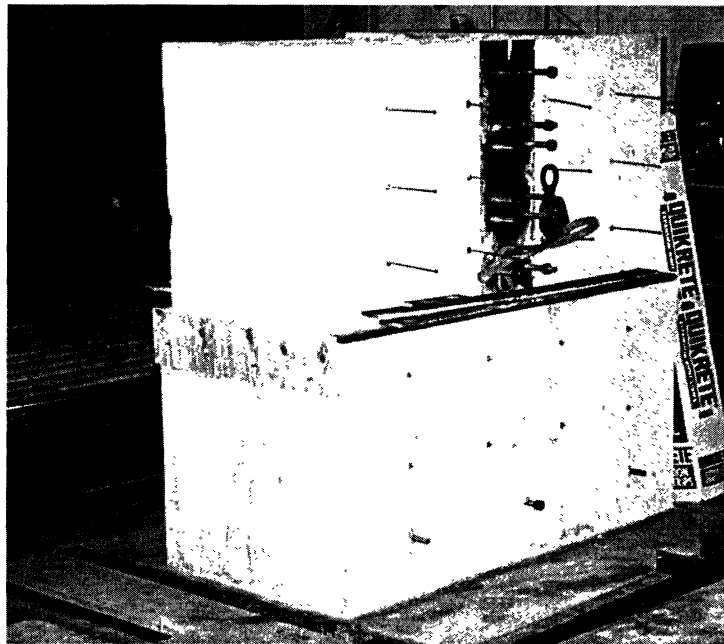
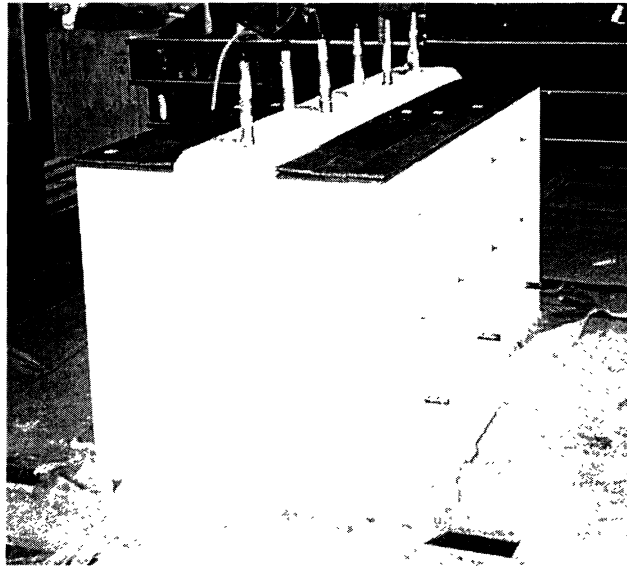


Figure 3. Pictures from construction of the initial VDOT integral abutment with hinge

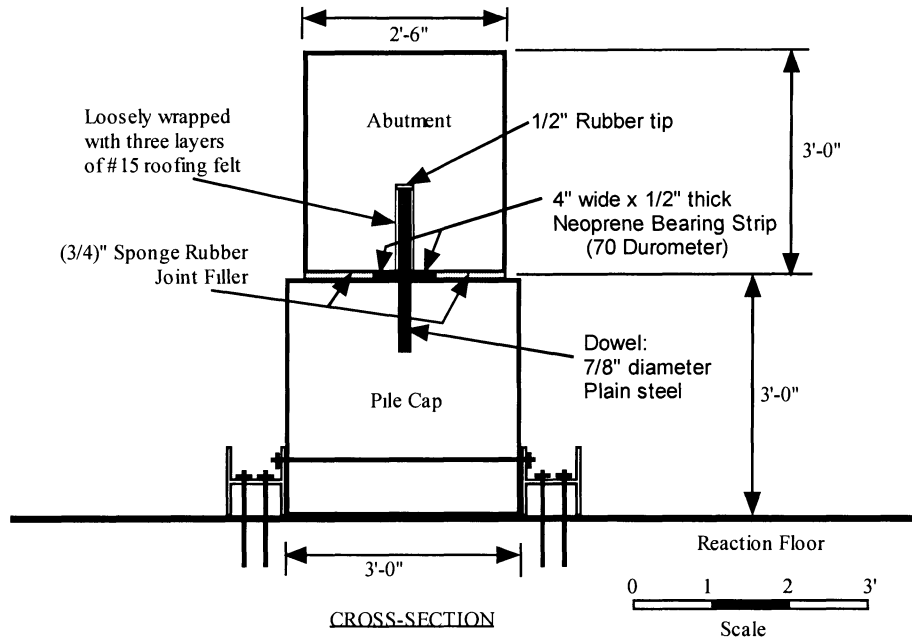


Figure 4. Schematic illustration of revised VDOT integral abutment with hinge

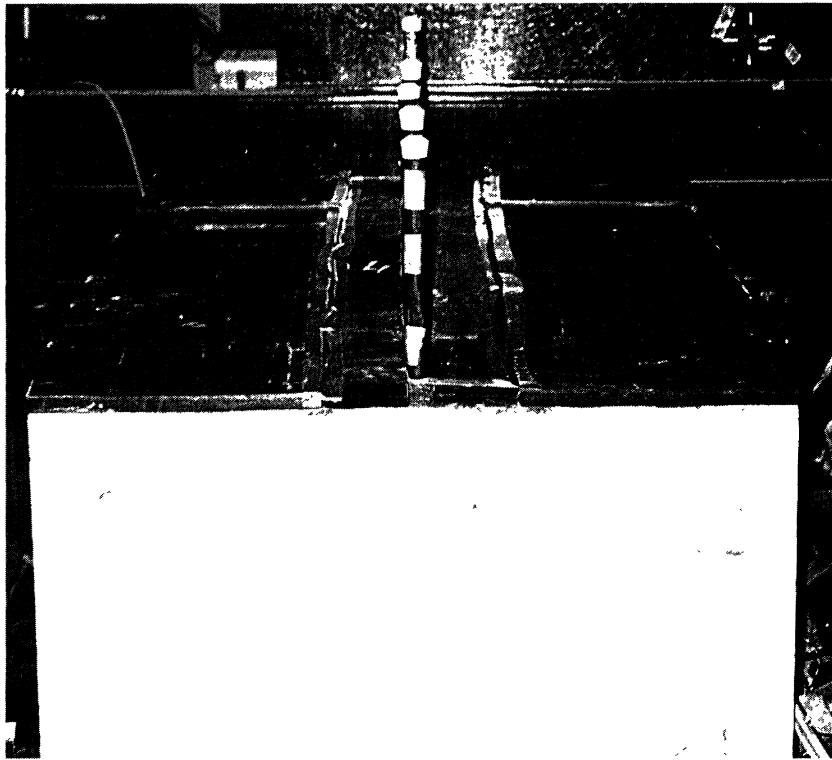


Figure 5. Picture from construction of revised VDOT integral abutment with hinge

## Material properties

### *Dowels*

The Charlotte steel mill of Ameristeel manufactured the dowels. They had yield and tensile strengths of 49,530 psi and 73,030 psi, respectively, as tested according to ASTM A36-94 by the manufacturer.

### *Concrete*

The specimens were cast from locally purchased VDOT Class A4 concrete. Concrete slump was checked for each batch received before placing the concrete. The slump varied from 3½ to 4 inches. Concrete samples from each batch were collected and compressive strengths of these samples were determined on the day of testing. Compressive strength of concrete for each member of the specimens is summarized in Table 2.

Table 2. Strength properties of concrete

Member	28-day strength (psi)	Age of concrete on test day (days)	Test-day strength (psi)
Specimen A – pile cap	5,970	69	6,920
Specimen A – abutment	6,400	58	7,740
Specimen B – pile cap	6,290	120	7,480
Specimen B – abutment	6,370	83	7,380
Specimen C – pile cap	6,290	196	7,800
Specimen C – abutment	5,530	10	4,420

## Load Test Setup

The setup of the load tests consisted of four tasks:

1. mounting the specimens onto the reaction floor
2. applying the vertical load
3. applying the lateral load in static loading
4. applying the lateral load in cyclic loading.

### *Mounting specimens on reaction floor*

Three threaded rods were placed in each pile cap during construction such that the rods extend out of the cap. On each side of a pile cap, an 8-foot segment of an HP10x42 was bolted on the threaded rods that were protruding from the pile cap. Figure 6 shows the locations of the

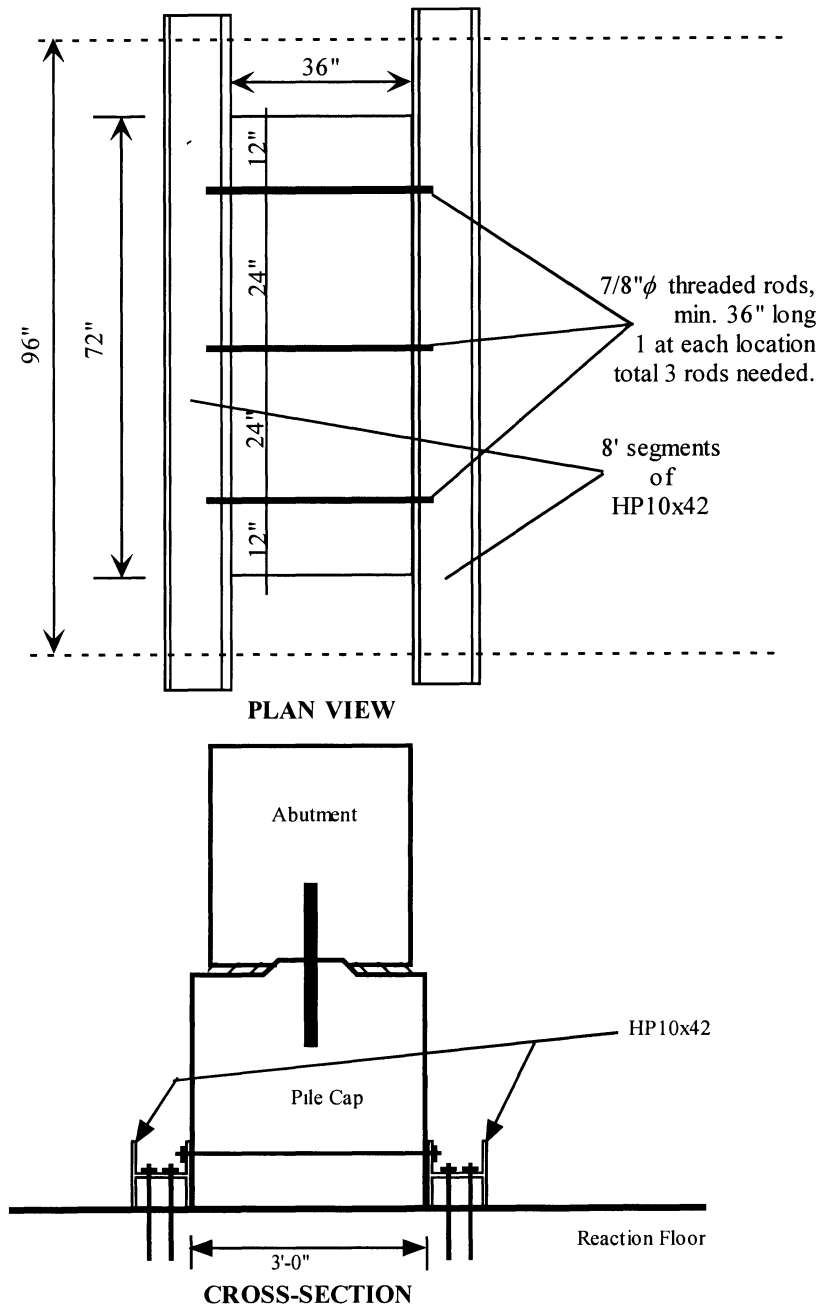


Figure 6. Schematic illustration of mounting pile caps on reaction floor

### *Application of vertical load*

The application of the vertical load was achieved through a specially designed system consisting of three components: (1) a stiff steel frame, (2) a single-acting hydraulic ram, and (3) a constant pressure valve.

The stiff steel frame was built around the specimens as pictured in Figure 7 to support the vertical loading ram. Loads were applied by a single-acting hydraulic ram. A compression load cell was placed between the frame and the ram.



Figure 7. Setup used to apply vertical load to specimens

As the lateral loads are applied and removed, the solid block rotates on its base and the top moves up or down under the ram. This up and down movement of the sample makes it impossible to maintain a constant vertical load if a standard ram is used. An Enerpac V-152 relief valve was used to maintain a constant load. The relief valve is designed to limit the applied load. The valve serves as a constant pressure valve by letting the pump run throughout the test. When the specimen rises under the ram, the valve relieves the extra pressure as soon as the maximum preset pressure is reached. When the abutment is lowered under the ram, the continuously running pump equilibrates the pressure to the preset pressure of the relief valve. The combination of using the relief valve and keeping the pump running allows maintaining the vertical load constant within  $\pm 10\%$  of the target value.

A roller and tilting-plate mechanism was placed between the top of the specimen and the vertical load ram to minimize the lateral load transfer at this location. A picture of this assembly is presented in Figure 8.

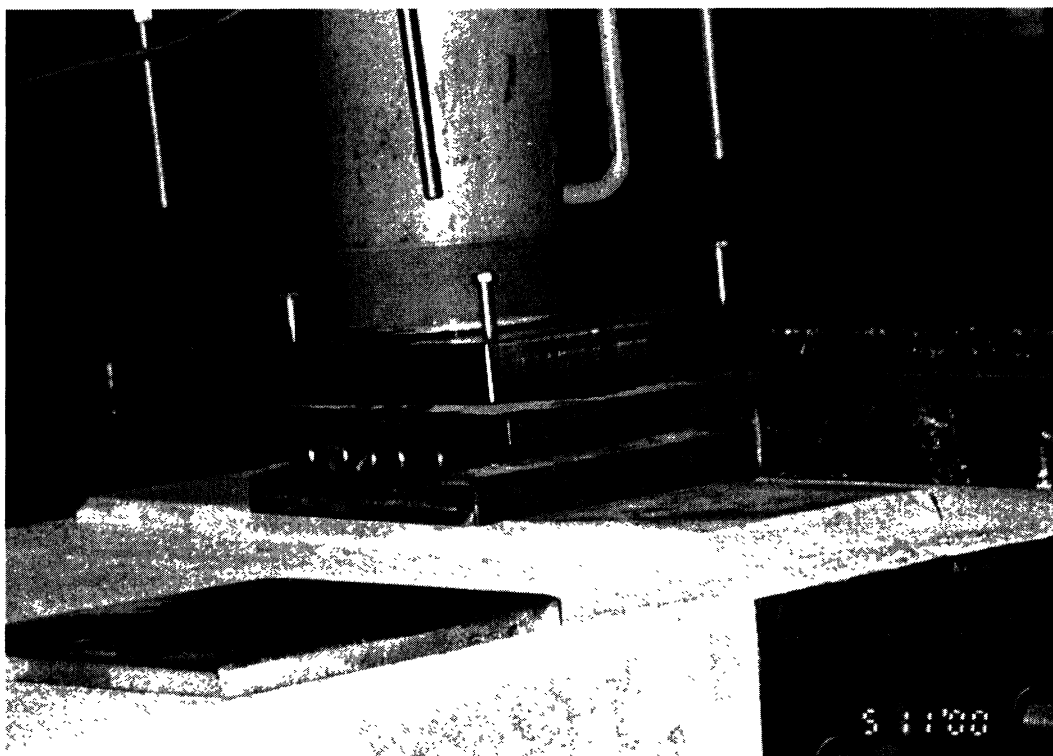


Figure 8. Roller and tilting-plate assembly used between ram and specimen

#### *Application of lateral load in static loading*

A manually controlled hydraulic ram capable of applying 50 kips of load was used to apply the static lateral loads. A view of the set up used is pictured in Figure 9. An A-shaped large stiff frame provided support for the ram. A 50-kip tension load cell was placed between the ram and the specimen to monitor the lateral load. The system was designed to pull only the specimen.

#### *Application of lateral load in cyclic loading*

A computer-controlled MTS hydraulic actuator capable of applying  $\pm 50$  kip of load and  $\pm 3$  inches of displacement was used to impose cyclic lateral loads. The same A-shaped large frame used in the static load tests provided support for the ram. A view of the actuator during testing is shown in Figure 10. The system was capable of applying both push and pull forces. The actuator can be used with either load or displacement control. A MTS 458.10 Micro Console unit provided actuator control with a 458.14 AC displacement controller, a 458.12 DC load controller, and a 458.90 function generator. All tests were run displacement controlled.

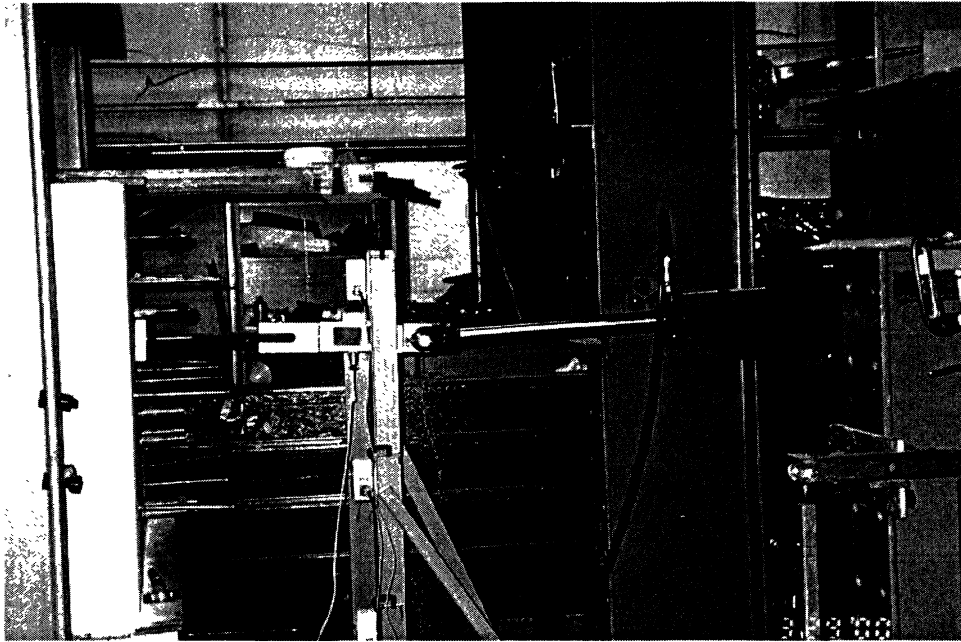


Figure 9. Setup used to apply static lateral load

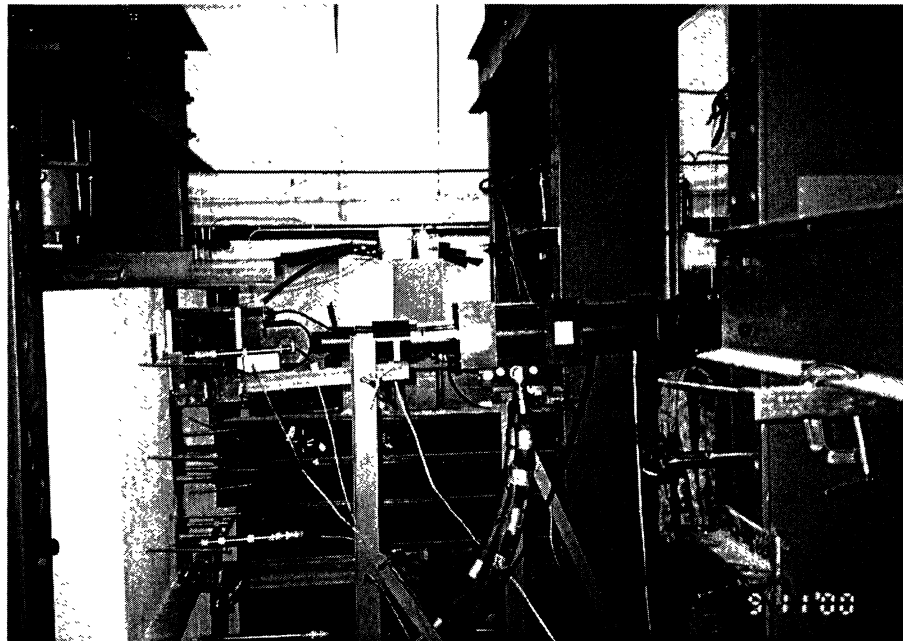


Figure 10. Setup used to apply cyclic lateral load

### *Instrumentation and Data Acquisition*

System 4000 marketed by the Measurements Group performed data acquisition during the static testing of Specimen A and Specimen B. The system includes a unit to read the analog voltage readings and to convert them into digital signals. The measurements are then stored into a personal computer.

Data from measuring devices during cyclic tests of Specimen B were collected into a MEGADAC 3108AC unit made by Optim Electronics. The unit converts the analog voltage readings from the measuring devices into digital signals. Digital signals are then sent to a PC, from which signals are read by the TCS data acquisition software. This setup was also used during the static and cyclic testing of the revised integral abutment with hinge (Specimen C).

Three types of measuring devices were used: (1) displacement, (2) load, and (3) strain. Displacement measurements were made by wire pot transducers. Each transducer was calibrated on-site immediately before it was put into service. Five transducers were used during each test. For convenience, the locations of the transducers were kept the same in all tests. Three of these transducers measured the lateral displacements of the abutment while the remaining two were used to record the vertical displacement of the abutment at the top. Figure 11 shows the locations of the displacement measuring devices.

In addition to displacement transducers, the MTS actuator has a built-in LVDT to measure the displacement of the actuator. Readings of this LVDT reflect the combined displacement of the abutment at the location where the load is applied and the displacement at the support of the actuator.

Two load cells were used: one for measuring the lateral load and one for measuring the vertical load. The lateral load cell used during cyclic loading was built into the MTS actuator. During static loading, a 50-kip tension load cell was used to monitor the lateral loads applied to the specimens. The vertical load cell was a compression load cell. Calibrations were checked before using these load cells, and no misreading was found.

Strain gages were purchased from the Measurements Group and installed according to the manufacturer's instructions. CEA-06-250UN-120 gages were used on steel dowel surfaces. The steel gages were  $\frac{1}{4}$  in long and had 120-ohm resistance with a gage factor of 2.065. The gages were placed on the opposite surface of each dowel instrumented to monitor bending stresses. The elevation of the strain gages was the same as the joint filler material. Four of the six dowels used per specimen were instrumented with strain gages for Specimens A and B. Two of the dowels of Specimen C were instrumented with strain gages.

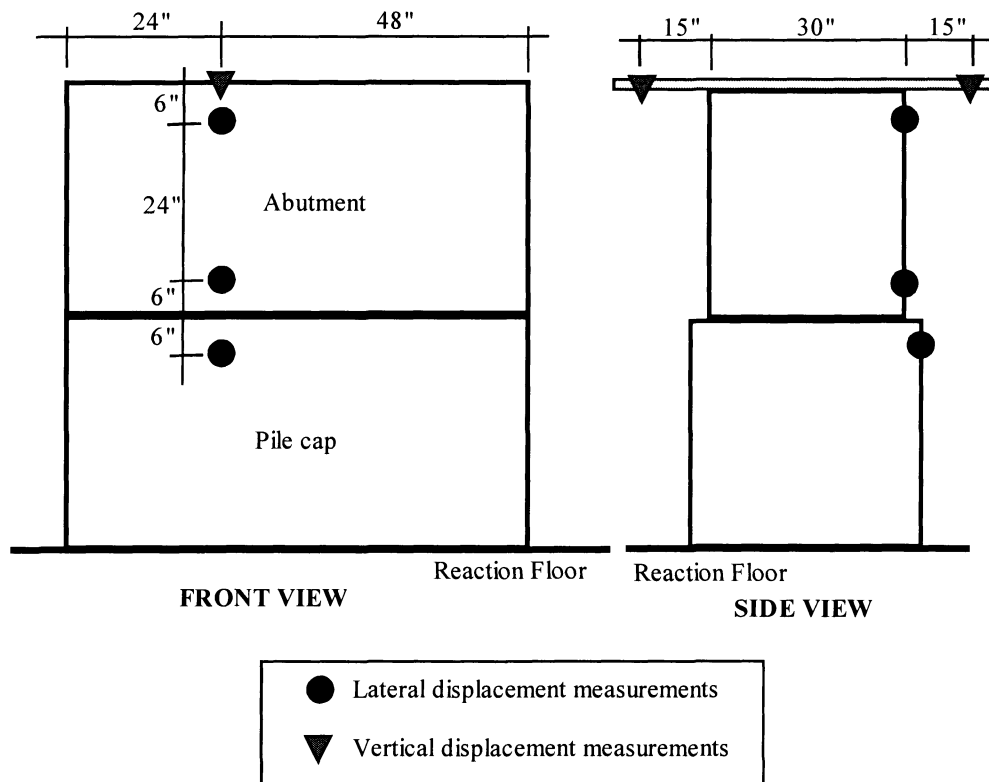


Figure 11. Locations of displacement measuring devices

## Test Program

### *Static Testing*

All three of the integral abutments with hinges were subjected to static lateral loading so that the top of the abutment displaced about an inch. A limit for the lateral load was set as 40 kips, which was imposed by the capacity of the load frame used to support the ram. The lateral loads were applied 5 inches below the top of the abutment or 31 inches above the abutment/pile cap joint. All three specimens were tested under vertical loads of 0, 35, and 70 kips.

As the lateral loads were applied to the specimens, the abutment rotated over the pile cap. Displacement transducers indicated that the pile caps also rotated slightly. The relative displacements of the abutments were calculated by subtracting the displacement readings measured at the top of the pile cap from the readings of the two displacement transducers used to monitor the displacements of the abutments at two different heights. By taking the average values of these two relative displacement values of the abutment and assuming a rigid behavior for the abutment, the relative displacement (with respect to the pile cap) at the top of the abutment was calculated.

Three additional tests were conducted on Specimen B by applying the lateral load 14 inches below the top of the abutment for vertical loads of 0, 35, and 70 kips.

In total, 12 static tests were conducted. The data obtained can be used to determine the rotational stiffness of the specimens.

*Application of displacement cycles*

Cyclic load tests were conducted on Specimens B and C for the purpose of simulating the effects of lateral loading induced by temperature changes over the expected life of the bridge. The life span of an integral bridge was considered to be 75 years.

Maximum displacements at the top of the abutment were set as  $\pm 0.5$  inch. Table 3 shows the displacement pattern used to simulate 75 years of thermal bridge displacements. Data collection was performed right after the 10<sup>th</sup>, 50<sup>th</sup>, and 75<sup>th</sup> years of simulated time. After the initial recording of data, 10 years of temperature effects were imposed according to the displacement pattern shown in Table 3. The number of displacement cycles in Table 3 was multiplied by 10 to simulate 10 years of loading. Forty more years of cyclic loading was imposed in the same manner. Finally, 25 more years of displacements were applied to complete the test.

Two vertical loads were used for each specimen: 0 and 35 kips. In total, four cyclic loading tests were conducted on two slightly different types of integral abutments.

Table 3. Representation of temperature-induced displacement cycles for 1 year for maximum expected displacement range from -0.5 to +0.5 inch

Group No	Corresponding days	Mean displacement level at the top of abutment (in)	Magnitude of cycles (in.)	Number of cycles for one year
1	0-46	-0.375	0.25	46
2	46-91, 320-365	-0.188	0.25	91
3	91-135, 270-320	0.000	0.25	91
4	135-180, 225-270	0.188	0.25	91
5	180-225	0.375	0.25	46
6	seasonal	0.000	1.00	1

**Experiments on Piles**

The main objective of this experimental program was to investigate the ability of three pile types to withstand cyclic lateral displacements induced by temperature variations. The pile types that were subjected to lateral loading in the laboratory were an H-pile, a pipe pile, and a prestressed reinforced concrete pile. The data from these tests were useful for selecting the type of pile best suited for supporting only integral bridges.

As the superstructure moves back and forth, the foundation piles of an integral abutment bridge are subjected to repeated cyclic loading. Maximum pile stresses take place near the pile cap. Experiments are conducted on a static equivalent of the pile/pile cap system to create maximum stresses near the pile cap. The equivalent system has upside down geometry of the pile/pile cap system under an integral bridge as illustrated in Figure 12. The orientation of the pile under an integral bridge is shown on the left-hand side of the figure. The equivalent pile/pile cap system is shown on the right hand side of the figure.

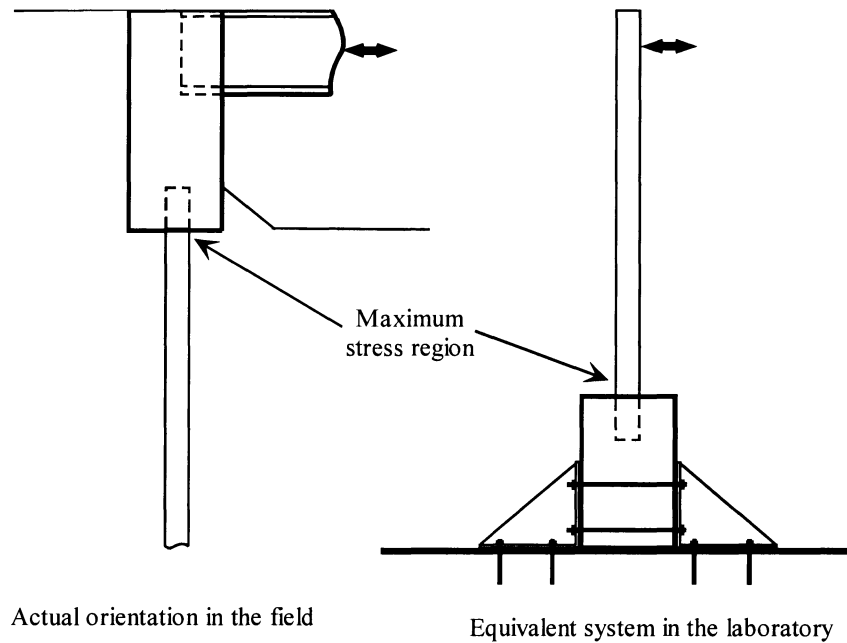


Figure 12. Static equivalent of pile/pile cap system in laboratory

### Design and Construction

Standard VDOT plans of integral abutment bridges were used to design the pile/pile cap samples. VDOT’s Staunton District provided the information necessary for design and reviewed the plans before advancing to construction. The pile specimens were constructed in the structures laboratory of Virginia Tech. Complete details of the experimental program can be found in Arsoy (2000).

The H-pile was cast into its cap on June 6, 2000. Construction of the pipe pile and the prestressed concrete pile were completed on June 16, 2000, and June 19, 2000, respectively. Concrete slump from each batch was checked before placing the concrete. The slump varied from 4 to 4¾ inches. Samples from each batch were taken to ensure proper strength on the test day.

## Material Properties

### Piles

The H-pile was an HP10x42 manufactured by Nucor-Yamato Steel of Houston, Texas. The heat ID and grade were 128775 and A572-50 S50, respectively. The pipe pile was made of ASTM A252 Grade 3 steel and had a 14-inch outer diameter and 0.5-inch wall thickness. The prestressed concrete pile was a 12-inch square standard VDOT pile. This pile had five ½-inch 270 ksi low relaxation steel strands. The prestress on the pile was 920 psi. Table 4 summarizes useful properties of the piles. These properties were compiled from material data sheets provided by the manufacturer for each pile.

Table 4. Properties of the piles used in the experiments

Pile type	Strength (ksi)*	Area (in <sup>2</sup> )	Moment of Inertia, I (in <sup>4</sup> )	Young's modulus, E (ksi)
H-pile	54.0	12.4	71.7	29,000
Pipe pile	45.0	21.2	484	29,000
Prestressed reinforced concrete	5.0	144	1,728	4,000**
* 28-day compressive strength for prestressed concrete pile, yield strength for steel piles				
** Determined by $E = 57,000\sqrt{f'_c}$ , where $f'_c$ = compressive strength of concrete (5,000 psi)				

### Concrete

Pile caps were cast from locally purchased VDOT Class A4 concrete. Because of the time constraints, early strength accelerators were added to concrete mixes of the caps for the pipe pile and the prestressed concrete pile. This additive produces the 28-day strength in about 7 days.

Concrete samples from each pile cap were collected, and compressive strengths of these samples were determined on the day of testing. Compressive strength and other useful properties of concrete for each pile cap are summarized in Table 5. Young's modulus of the concrete is calculated by  $E = 57,000\sqrt{f'_c}$ , where  $f'_c$  is the strength on the test day in psi.

Table 5. Strength properties of concrete of pile caps

Pile type	Age on test day (day)	Strength on test day (psi)	Slump (in.)	Young's modulus, E (ksi)
H-pile	18	4,200	4	3,700
Pipe pile	11	4,500	4 ¾	3,800
Prestressed concrete	11	4,500	4 ¾	3,800

## Load Test Setup

The setup of the load tests consists of three major tasks:

1. mounting pile cap onto the reaction floor
2. applying the vertical load to the pile
3. applying the lateral load to the pile.

### *Mounting pile caps on reaction floor*

Six threaded rods were placed in each pile cap during construction such that the rods extended out of the cap. On each side of a pile cap, an 8-foot segment of an HP10x42 was bolted on the threaded rods that were protruding from the pile cap. Figure 13 shows the locations of the threaded rods and the floor-mounting plan of the pile caps. The HP10x42 segments were bolted down to the reaction floor at each corner by specially made L-shaped steel elements as pictured in Figure 14. Four of these elements were used for each pile cap.

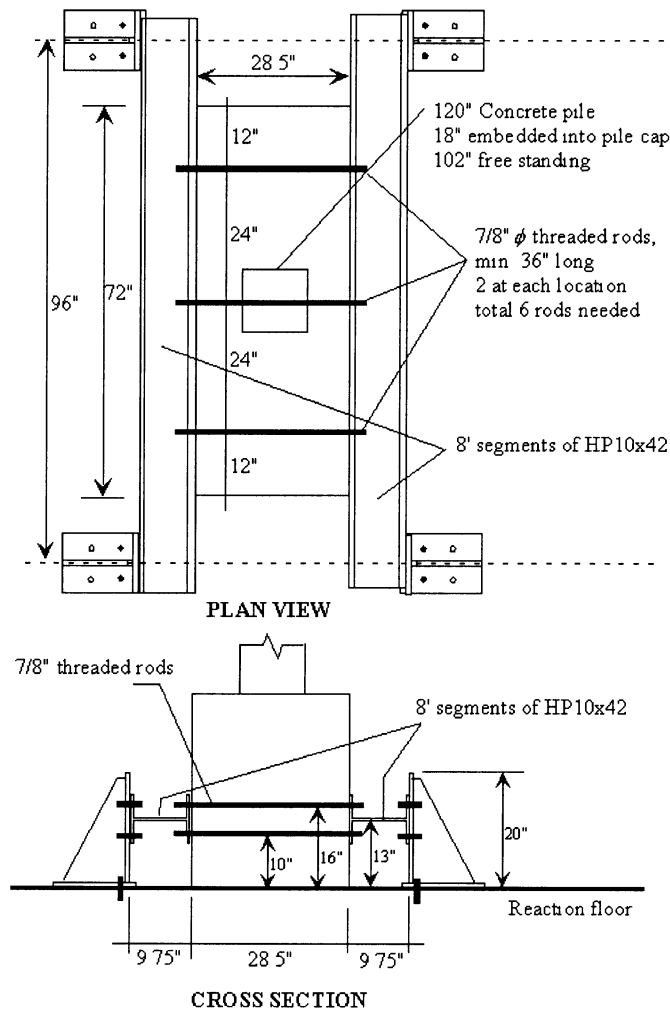


Figure 13. Schematic of mounting pile caps on reaction floor

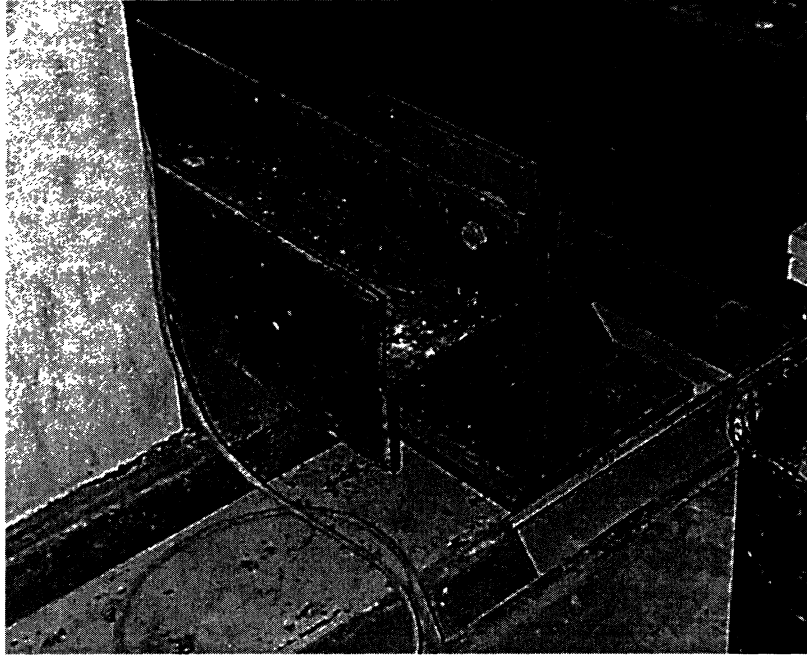


Figure 14. Mounting pile caps to reaction floor by L-shaped steel elements

### *Application of vertical load*

The application of the vertical load was achieved through a specially designed system. The system consists of three components, as can be seen in Figure 15: (1) steel beam, (2) two hydraulic rams, and (3) two support elements called gravity load simulators (GLS).

The steel beam was first bolted on the top of the pile to be tested. Then the rams were hung by pins from each corner of the beams. The other ends of the rams were connected to the middle pin of the GLS as seen in Figure 15. A GLS is a simple frame that has five pinned connections. These pins are located on each corner of the GLS.

The unique structure of the gravity load simulators and the pinned connections of the hydraulic rams keep the rams vertical for any given lateral displacement of the pile being tested. A tension load cell was also placed between each ram and each GLS.

Both of the rams were controlled by a single pump to ensure even distribution of the vertical load on each side of the top beam. Each ram provided half the vertical load acting on the pile.

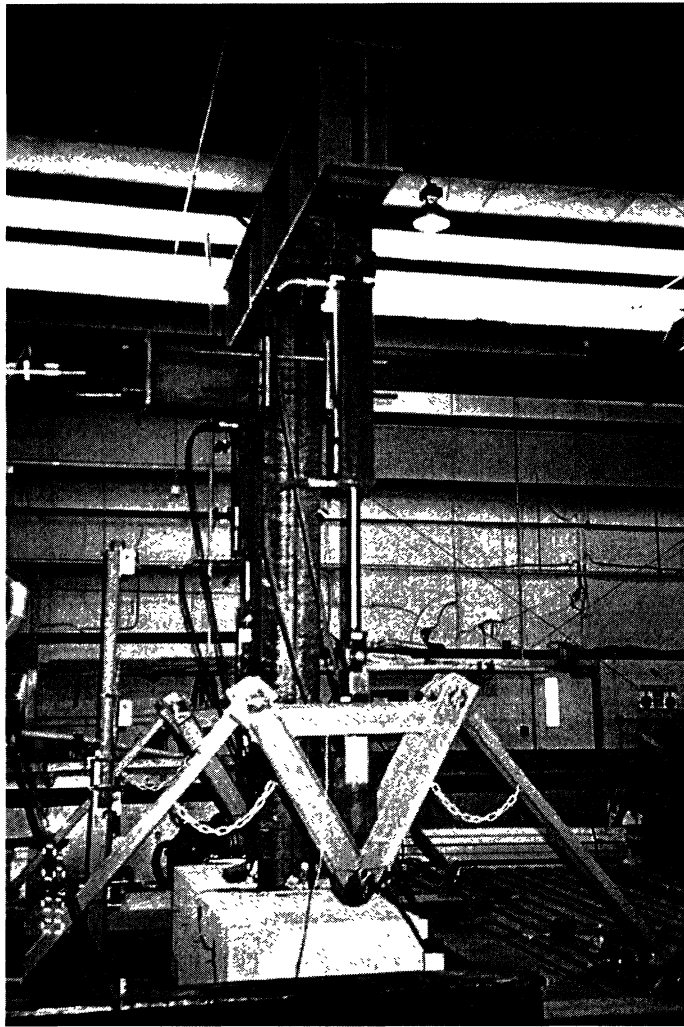


Figure 15. Vertical load application to piles

### *Application of lateral load*

A computer-controlled MTS hydraulic actuator capable of applying  $\pm 50$  kips of load and  $\pm 3$  inches of displacement was used to apply cyclic lateral loads. Views of the actuator during testing are shown in Figure 16.

The actuator can be used as either load or displacement controlled. Actuator control is provided by an MTS 458.10 MicroConsole unit with a 458.14 AC displacement controller, a 458.12 DC load controller, and a 458.90 function generator. All tests were run displacement controlled.

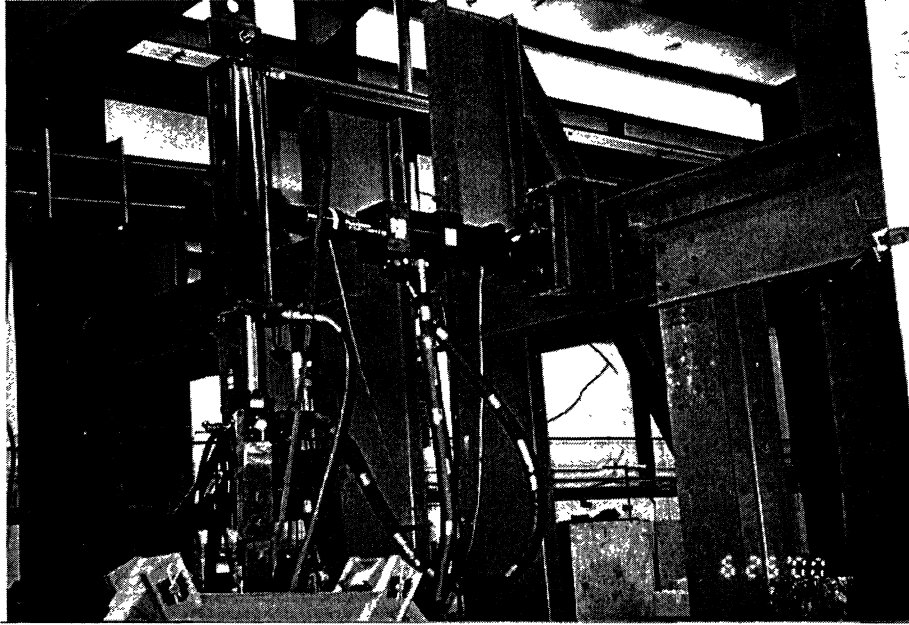


Figure 16. View of the MTS actuator during cyclic lateral loading

*Instrumentation and data acquisition*

Piles were tested using the same equipment as was used for the abutments. Lateral pile displacements were measured 7, 28, and 53 inches above the pile cap. Figure 17 shows a picture of a steel stand placed on the pile cap. This steel stand was placed in the middle of the pile cap. Two transducers measured the displacements of the steel stand at two locations: 4 and 13 in above the pile cap. The data from these two transducers were used to calculate the rotation of the pile cap.

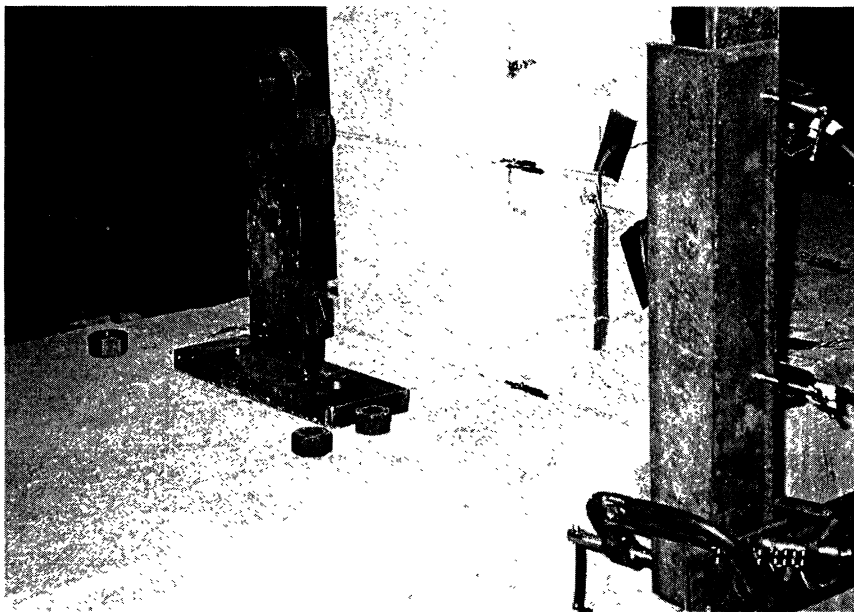


Figure 17. Picture of steel stand used to measure rotation of pile cap

The locations of the strain gages are shown in Figure 18. The H-pile had four gages near the pile cap: two were located at the opposite tips of the flanges, and the other two were used as backup near the tip of the flanges. The pipe pile had four gages: two were located near the pile cap, one was located 55 inches above the pile cap, and the last one was located 70 inches above the pile cap. The prestressed concrete pile had two gages, both of which were placed near the pile cap on the opposite sides of the pile.

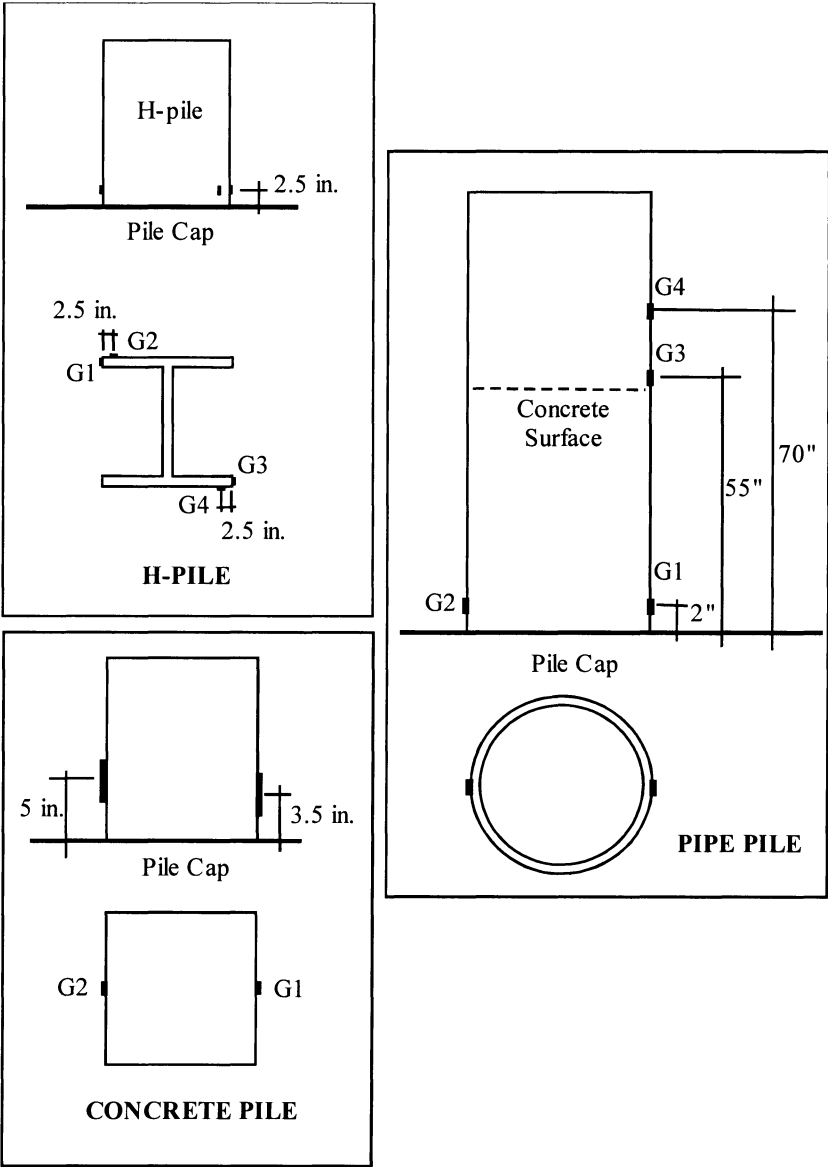


Figure 18. Locations of strain gages used in experiments on piles

## Test Program

The purpose of the test program was to simulate the effects of lateral loading induced by temperature changes over the expected life of integral bridges and evaluate damage to the pile/pile cap system under working stress conditions. The life span of an integral bridge is deemed to be 75 years. Approximately 27,000 small cycles are necessary for a 75-year simulation of bridge life. To input this many cycles, one would like to use the highest excitation frequency possible. Before setting the excitation frequency, natural frequencies of each pile were calculated using Equation 1 (James et al., 1994).

$$f_n = \frac{1}{2} \sqrt{\frac{g}{W} \left( \frac{EI\pi^2}{32l^3} - \frac{W}{8l} \right)} \quad (\text{Equation 1})$$

Where,

- $f_n$  = natural frequency of the pile
- $g$  = acceleration of the earth
- $W$  = weight of each pile plus any vertical load
- $l$  = length of each pile (102 inches).

Table 6 shows the natural frequency calculated for each pile for a vertical load of 70 kips. For smaller vertical loads, the natural frequency is higher.

As the excitation frequency approaches to the natural frequency in a load-controlled test, displacements become larger. These large displacements can result in an unintended failure of the pile because of the resonance phenomenon. If the excitation frequency remains below 25% of the natural frequency, displacements remain very close to those resulting from static loading (James et al., 1994). Because the experiments are displacement controlled, it is possible to set the excitation frequency higher than 25% of the natural frequency. The final decision of the excitation frequency was made after several trial runs under various vertical loads. It was found that there is some amplification of displacements for frequencies above 0.7 Hz for the H-pile. The operating frequency was set as 0.6 Hz for small cycles for all pile types. For the large cycles, the excitation frequency was selected as 0.1 Hz.

Table 6. Estimated natural frequencies of piles for 70 kips of vertical load

Pile type	$f_n$ , Natural frequency (Hz)
Steel HP10x42	0.85
Pipe pile	2.35
Prestressed reinforced concrete	1.54

### Steel H-pile

The designation of the experiments and a brief description of each are indicated in Table 7. In test HP-BB, the maximum stress level was targeted as 50% of the nominal yield capacity of the pile. The test was run displacement controlled. Strain gage readings were collected before testing the pile in order to determine the relationship between the displacement at the top of the pile and the maximum stress in the pile. Subsequently, the displacement of the MTS ram was set to generate the target stress level.

Table 7. Description of the tests conducted on the steel H-pile

Designation	Description
HP-AA	Application of 75 major cycles on the H-pile. Maximum target stress: $\pm 17$ ksi.
HP-BB	Simulation of 75-year temperature variations by 75 large cycles and 27,375 smaller cycles following test HP-AA. Maximum target stress: $\pm 17$ ksi.
HP-CC	Application of 75 major cycles on H-pile following test HP-BB. Maximum target stress: $\pm 17$ ksi.
HP-DD	Attempting to fail the H-pile by using the maximum displacement stroke of the hydraulic actuator.

Table 8 summarizes the representation of a year of temperature variations in the experiments. For each year of the bridge life, a large displacement cycle and 365 small daily cycles were imposed on the pile. The large displacement cycle represents the maximum temperature variation seen in 1 year. The smaller daily cycles are in three groups representing spring and fall combined, summer, and winter variations. Approximately one third of the maximum displacements were used to simulate daily temperature variations.

Table 8. Representation of one year of temperature effects in the laboratory

Cycle designation	Targeted stress range (ksi)	Mean stress level (ksi)	Excitation frequency (Hz)	Number of cycles
HP-L1	-17 to +17	0	0.1	1
HP-S1	-8 to +8	0	0.6	183
HP-S2	0 to +17	8.5	0.6	91
HP-S3	-17 to 0	-8.5	0.6	91

### Steel Pipe Piles

The load frame was designed for a smaller diameter pipe pile than the 14-in pipe pile supplied by the project sponsor. Therefore, the test system was capable of imposing only 6 ksi of axial stress in the pipe pile instead of the targeted 17 ksi. Further, the connection between the pipe pile and the pile cap, consisting of a steel reinforcing cage embedded 5 ft into the pipe pile

filled with concrete (Arsoy, 2000), was much stiffer than in the other piles tested. This resulted in limited flexibility of the connection and the inability of the attachment to the reaction floor to prevent rocking of the pile cap, and only about 2300 cycles at 0.1 Hz. were imposed. As a result, only limited conclusions can be drawn comparing the pipe pile performance with other pile types.

### *Prestressed Reinforced Concrete Pile*

Effects of the temperature variations were modeled similar to the H-pile test. Three series of experiments were conducted: CP-AA, CP-BB, and CP-CC. Designation of the experiments and a brief description of each are provided in Table 9. Table 10 summarizes the representation of a year of temperature variations in the experiments.

Table 9. Description of the tests conducted on the concrete pile

Designation	Description
CP-AA	Application of 150 major cycles on prestressed concrete pile. Maximum target stress: 2.5 ksi.
CP-BB	Simulation of 75-year temperature variations by 75 large cycles and 27,375 smaller cycles following test CP-AA. Maximum target stress: 2.5 ksi.
CP-CC	Application of 75 major cycles on prestressed concrete pile following test CP-BB. Maximum target stress: 2.5 ksi.

Table 10. Representation of 1 year of temperature effects in the laboratory

Cycle designation	Targeted stress range (ksi)	Mean stress level (ksi)	Excitation frequency (Hz.)	Number of cycles
CP-L1	-2.50* to +2.50	0	0.1	1
CP-S1	-1.25* to +1.25	0	0.6	183
CP-S2	-1.25* to 0.00	-0.625*	0.6	91
CP-S3	0.00 to +1.25	+0.625	0.6	91

\*Because of tension cracks, concrete does not experience this tension stress.

### **Numerical Analysis**

Integral bridges are subjected to complex soil/structure interactions. A thorough understanding of these interactions is needed to provide a basis for expanding the current limits on the lengths of integral abutment bridges.

## **Soil/Abutment/Pile Interactions**

As the superstructure expands toward the approach fill, a series of interactions takes place between the following components of the bridge and its foundation:

- abutment/approach fill
- approach fill/foundation soil
- foundation soil/pile
- pile/abutment.

Abutment/approach fill interactions result in changes in the earth pressures acting on the bridge abutment. The magnitude and the mode of the abutment movement are primary factors that control the earth pressures. Earth pressures decrease as the bridge contracts and increase when the bridge expands (see Arsoy, Barker, and Duncan, 1999, for more information).

As the approach fill is pushed by the abutment, it tends to move the foundation soil in the same direction. This is beneficial as far as the pile stresses are concerned because the foundation soil acts as if it were softer because it is moving in the same direction as the piles. This results in lower stresses in the piles.

The type of foundation soil is important in determining the pile stresses. For conditions where a given amount of displacement is imposed at the tops of the piles, as is the case for piles supporting integral bridges, softer soils result in lower pile stresses than do stiffer soils. A computer program such as LPILE is useful for assessing the stresses resulting from imposed displacements.

## **Software Selection**

The interactions between the bridge system and the approach system would be best modeled by a finite element program capable of solving three-dimensional problems. However, 3D finite element analyses would require more time and effort than was possible within the budget of this study. For many years, two-dimensional analyses have been used widely for soil-structure interaction problems and have proven adequate for design studies. Therefore, it was decided to use the 2D computer programs SAGE and LPILE for this investigation.

### *SAGE*

Finite element analyses were performed using the finite element program SAGE 2.03 (Static Analysis of Geotechnical Engineering Problems) developed at Virginia Tech. SAGE is capable of analyzing 2D plane strain soil-structure interaction problems. Newton-Raphson iteration is used to solve the non-linear equations.

Element types include triangular, quadrilateral, beam-bar, Wilson, and zero-thickness interface elements. Soil behavior can be modeled by choosing from ten material models, including; Mohr-Coulomb, Drucker-Prager, Hyperbolic, and Cam Clay (Bentler et al., 1999).

### LPILE

LPILE is a program developed by Ensoft, Inc. of Austin, Texas, for analyzing the behavior of piles under lateral loading. The program is based on the finite difference method and approximates 3D soil/pile interaction through the use of nonlinear p-y curves.

Deflection, shear, moment, and soil response along the pile are computed. The boundary conditions at the pile head can be specified in terms of shear, moment, displacement, and rotational stiffness.

### Bridge Geometry

A typical 300-ft long integral abutment bridge was selected for the parametric analyses. The bridge consists of W44x285 steel girders spaced 8 ft apart, with a 10-in-thick concrete deck resting on 10-ft-high 3.0-ft-thick abutments, which are supported by HP10x42 steel piles, spaced 6 ft apart, as shown in Figure 19.

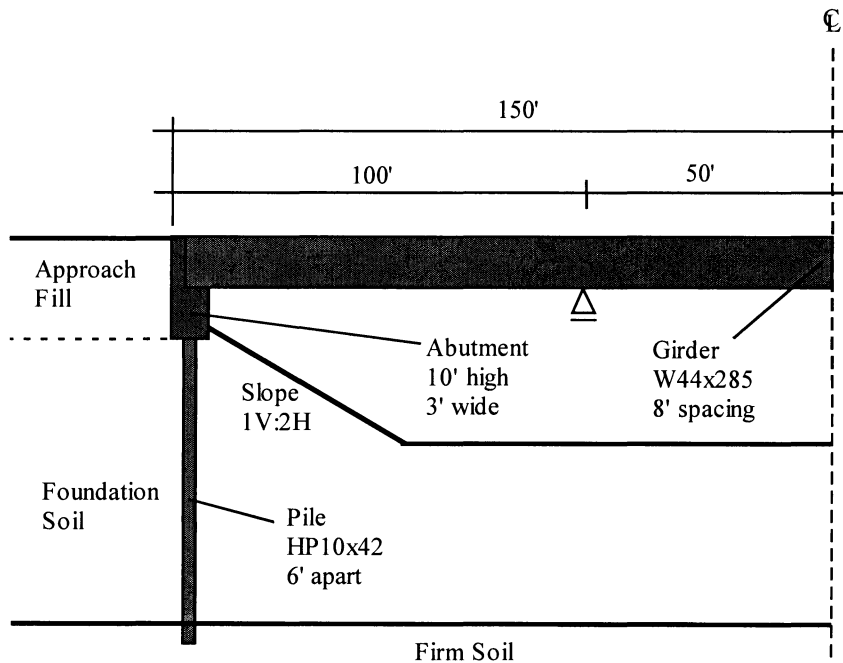


Figure 19. Geometry of bridge considered in finite element analyses

Two abutment types were considered: full integral and integral with hinge. Enlarged views of these abutments are depicted in Figure 20. The integral abutment with hinge is similar

to a full integral abutment, except for a lateral joint in the middle of the abutment. A dowel passes through this joint to prevent shear displacements between the top and bottom sections of the abutment.

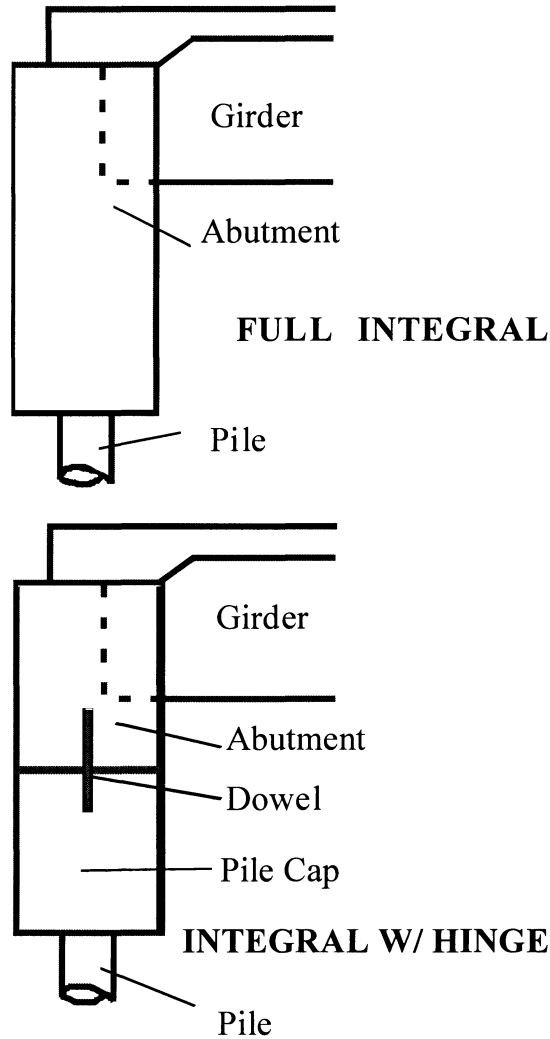


Figure 20. Enlarged views of full integral and integral with hinge abutment details

The bridge was modeled as a plain strain problem, with symmetry around the centerline of the bridge. The finite element mesh used in the analyses is shown in Figure 21. Both the full integral and the integral with hinge abutments were modeled using the same mesh. As can be seen in Figure 21, the mesh is finer around the abutment and coarser near the boundaries. Zero-thickness interface elements were used between the approach fill and the abutments.

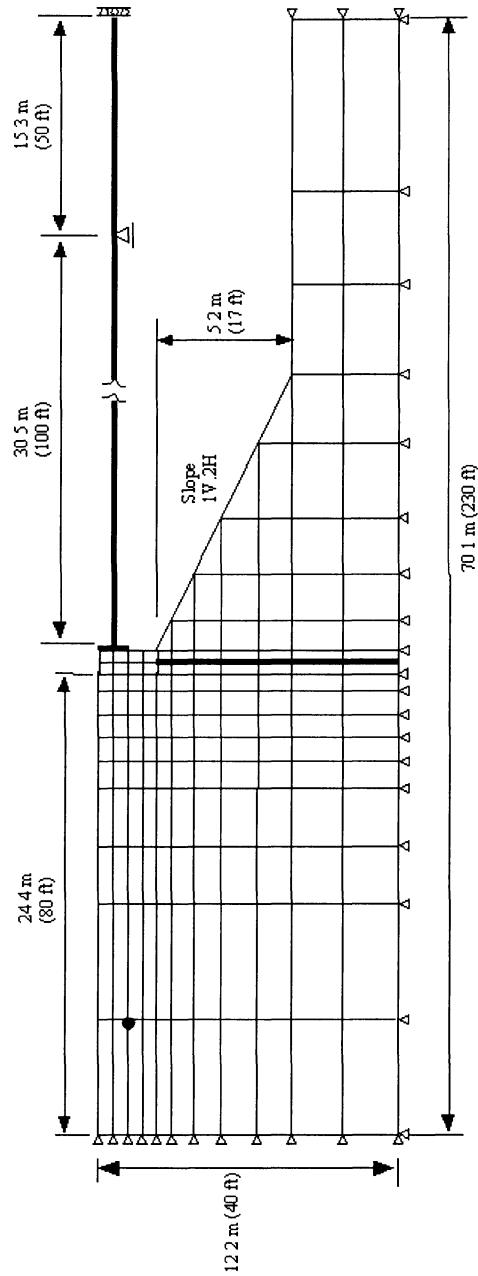


Figure 21. Finite element mesh used for the bridge analyzed

Sections of the finite element mesh around the full integral abutment and the integral abutment with hinge are shown in large scale in Figures 22 and 23, respectively. The lateral joint in the integral abutment with hinge was modeled by quadrilateral elements and beam-bar elements as shown in Figure 23.

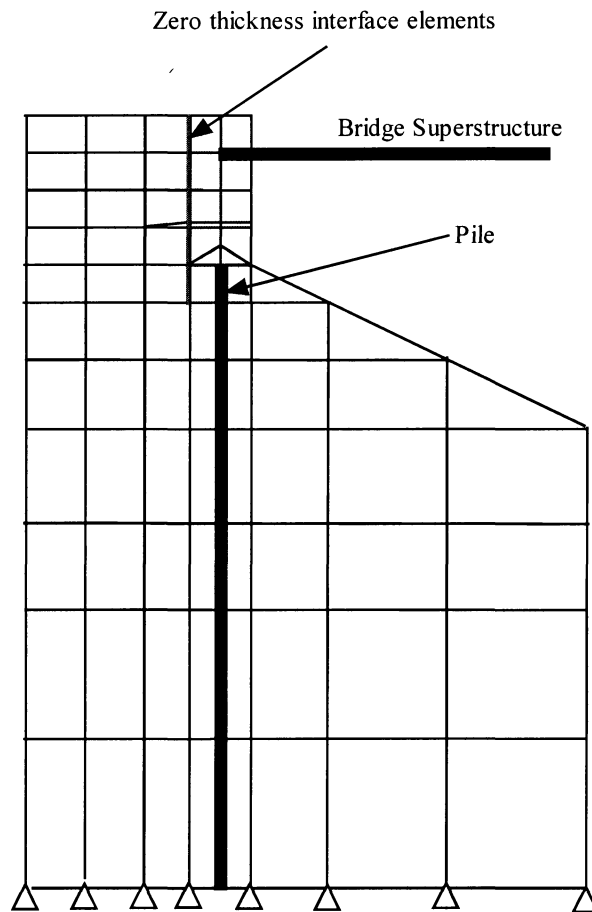


Figure 22. Finite element mesh of area around full integral abutment

### Material Properties

Different types of models of nonlinear soil behavior are used in SAGE and LPILE. The parameters used in these analyses were obtained from published literature (Duncan et al., 1980; Reese and Wang, 1997).

#### *SAGE*

The bridge superstructure, the piles, and the dowels of the integral abutments with hinges were modeled as beam-bar elements with linear stress-strain properties. The abutment and the joint-filler in the integral abutment with hinge were modeled using four-node quadrilateral elements with linear stress-strain properties. The approach fill and the foundation soil were modeled using four-node quadrilateral and three-node triangular elements with hyperbolic

material properties. Tables 11 and 12 summarize the material properties used in the analyses. The hyperbolic soil parameters representing dense to loose sand were selected from Duncan et al. (1980).

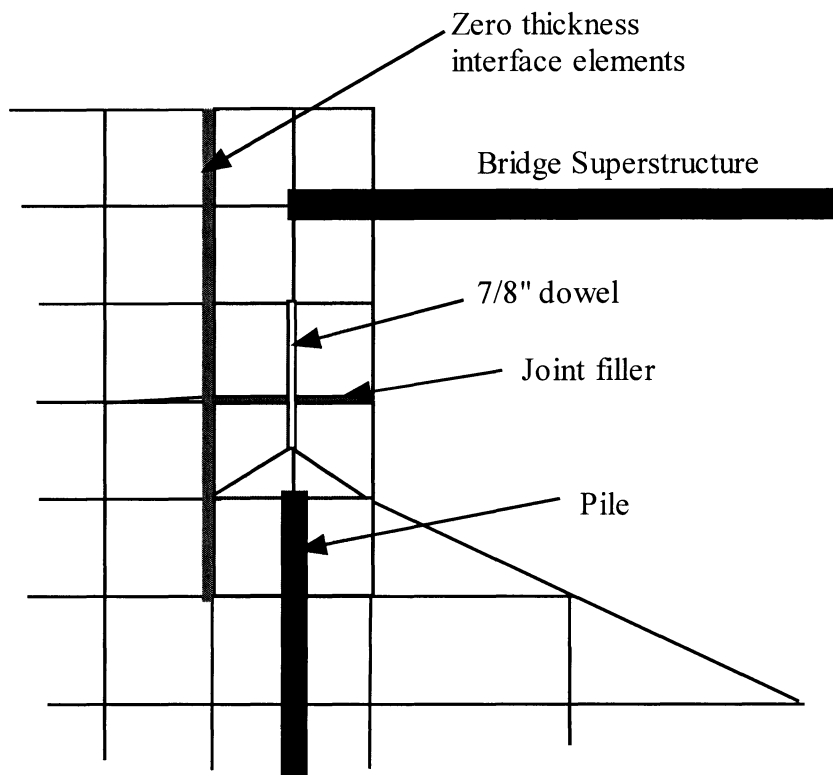


Figure 23. Finite element mesh of area around integral abutment with hinge

The behavior of the joint-filler was modeled by setting the values of modulus for these elements approximately equal to zero so that it would not contribute to the shear and all the shear force would be absorbed by the dowels.

### *LPILE*

Table 13 summarizes the soil parameters used in LPILE. These values were obtained from the program manual (Reese and Wang, 1997). The soil parameters shown in Table 13 were used by LPILE to generate the  $p$ - $y$  curves used in the analyses.

### **Assumptions and Sources of Errors in Numerical Modeling**

A comparative study was made to determine the degree of correspondence between the results of laterally loaded pile analyses performed with SAGE and with LPILE. Three soil conditions (dense, medium dense, and loose sand) and two boundary conditions (fully fixed and partially fixed head) were considered. The properties of the steel HP10x42 piles and the soil used in the analyses are listed in Tables 11, 12, and 13.

Table 11. Properties of structural components

Structural Component	Bridge beams	Pile	Dowels
EA (kips)	$2.43 \times 10^6$	$0.36 \times 10^6$	$17.4 \times 10^3$
EI (kips-ft <sup>2</sup> )	$4.95 \times 10^6$	$14.44 \times 10^3$	11.58
Spacing (ft)	8	6	1
EA per ft. (kips/ft)	~0*	$60 \times 10^3$	$17.4 \times 10^3$
EI per ft. (kip-ft <sup>2</sup> /ft)	$600 \times 10^3$	$2.4 \times 10^3$	11.58
*Axial loads in the beams were not of concern (see section 6.8 for details)			

Table 12. Hyperbolic stress-strain and strength parameters for approach fill and foundation soils

Parameter	Loose Sand	Medium Dense Sand	Dense Sand
$\gamma$ , Unit weight (pcf)	115	125	140
c, Cohesion	0	0	0
$\phi$ , Friction angle (degrees)	33	36	42
$R_f$ , Failure ratio	0.7	0.7	0.7
K, Young's modulus coefficient	200	300	600
n, Young's modulus exponent	0.4	0.4	0.4
K, Bulk modulus coefficient	50	75	175
M, Bulk modulus exponent	0.2	0.2	0.2

A total of six analyses were conducted as tabulated in Table 14. The slope at the pile head was assumed to be either 0 or 0.005, which brackets the range expected for most piles supporting integral abutment bridges.

Table 13. Parameters used to define  $p$ - $y$  curves in LPILE

Parameter	Loose Sand	Medium Dense Sand	Dense Sand
$\gamma$ , Unit weight (pcf)	115	125	140
$c$ , Cohesion	0	0	0
$\phi$ , Friction angle (degrees)	33	36	42
$k$ , coefficient of horizontal subgrade reaction (lb/in <sup>3</sup> )	25	90	225

Table 14. Comparison of Shear and Moment as calculated by SAGE and LPILE

Case No.	Soil Type	Top Slope (rad)	Top Deflection (in.)	Shear <sub>LPILE</sub> / Shear <sub>SAGE</sub>	Moment <sub>LPILE</sub> / Moment <sub>SAGE</sub>
D-FF	Dense	0	0.69	1.05	1.51
D-PF	Dense	0.005	0.69	0.81	1.45
MD-FF	Medium Dense	0	0.44	1.10	1.41
MD-PF	Medium Dense	0.005	0.52	0.87	1.52
L-FF	Loose	0	0.71	1.05	1.31
L-PF	Loose	0.005	0.70	0.87	1.37

D = dense sand, MD = medium dense sand, L = loose sand  
 FF = fully fixed = zero rotation at the top of the pile  
 PF = partially fixed: rotation = 0.005 radians at the top of the pile

Comparisons of the solutions by SAGE and LPILE were made for deflection, shear, and bending moment. Table 14 shows that the results of the SAGE analyses compare reasonably well with the results of the LPILE analyses (consult Arsoy, 2000, for details). Although the piles supporting the abutment must be represented as equivalent two-dimensional piles in such analyses, the computed results can be expected to be qualitatively the same, and quantitatively similar, to the actual three-dimensional behavior, at least as judged by the correspondence between the SAGE and LPILE results shown in Table 14.

## RESULTS

### Abutment Experiments

#### Static Load Tests

In the first static test of Specimen A, the shear key of the specimen failed with a loud noise. At the time of the failure, the lateral was about 34 kips applied 29 inches above the shear key.

No vertical load was applied to the sample other than its self-weight. A picture of the failed shear key is shown in Figure 24.

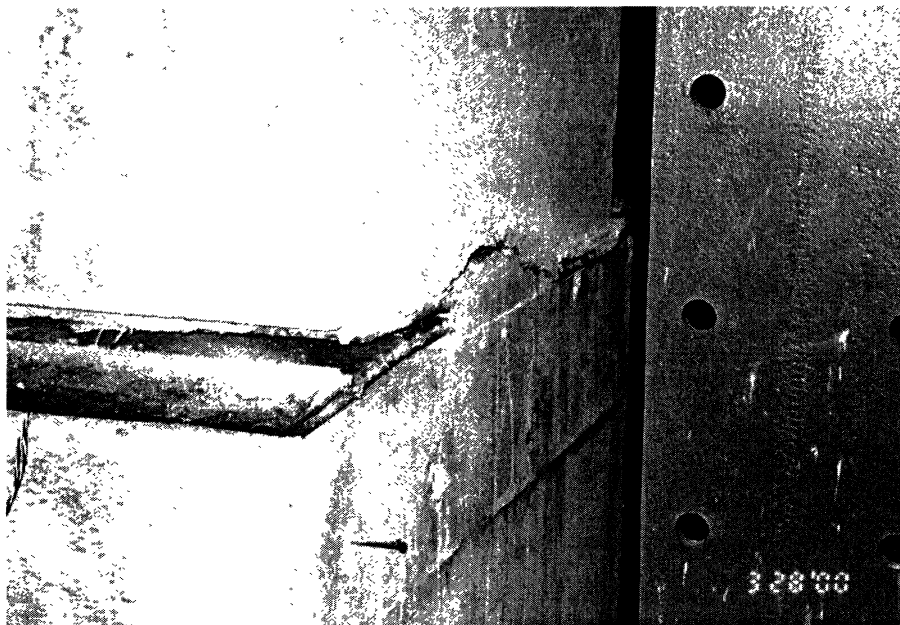


Figure 24. Picture of failed shear key

Analysis of the data indicated that the abutment and the pile cap rotated as a single structural unit prior to failure of the shear key. This suggests that the cold bond between the pile cap and the abutment was as strong as if they were cast together. The lateral load at the time of failure was calculated to generate a tensile stress of about 550 psi in the concrete of the shear key. This stress was within the estimated tensile strength range of the specimen.

Specimen B was tested under the same conditions as the first specimen. The failure of the shear key took place in a similar manner when the lateral load reached about 34 kips applied 28 inches above the shear key. Tensile stresses generated by the lateral load were within the tensile strength range of the concrete.

The failure of the shear key was due to concrete of the shear key failing in tension because of bending. Static load tests conducted after the shear key failure found that both abutments were able to provide shear resistance, indicating that the dowels did not fail and the failure was limited to the concrete of the shear key. Unfortunately, all of the strain gages were lost at the time the shear key failed.

The relationship between the lateral load and the relative displacement at the top of the abutment is shown in Figures 25 and 26. Three levels of vertical loading were applied on the abutments to simulate the dead load of the bridge. As seen in the figures, the loading/unloading curves for the original integral abutment with hinge (A and B) were much closer to each other than the loading/unloading curves of the revised detail (C).

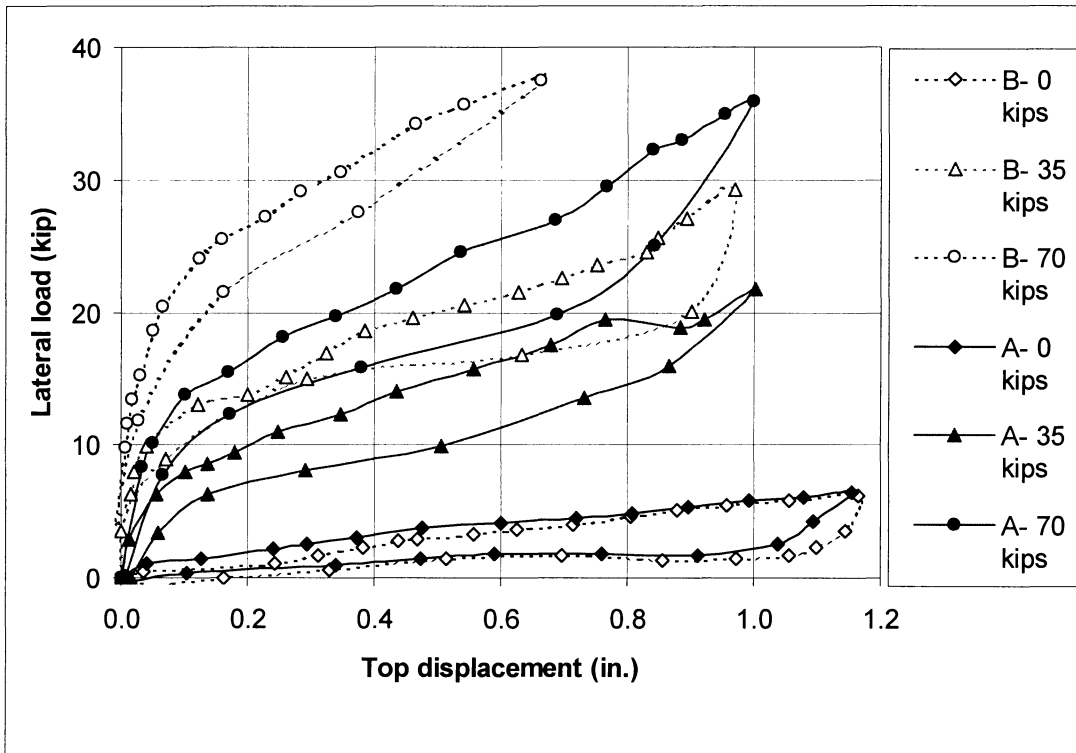


Figure 25. Lateral load/displacement relations of Specimens A and B

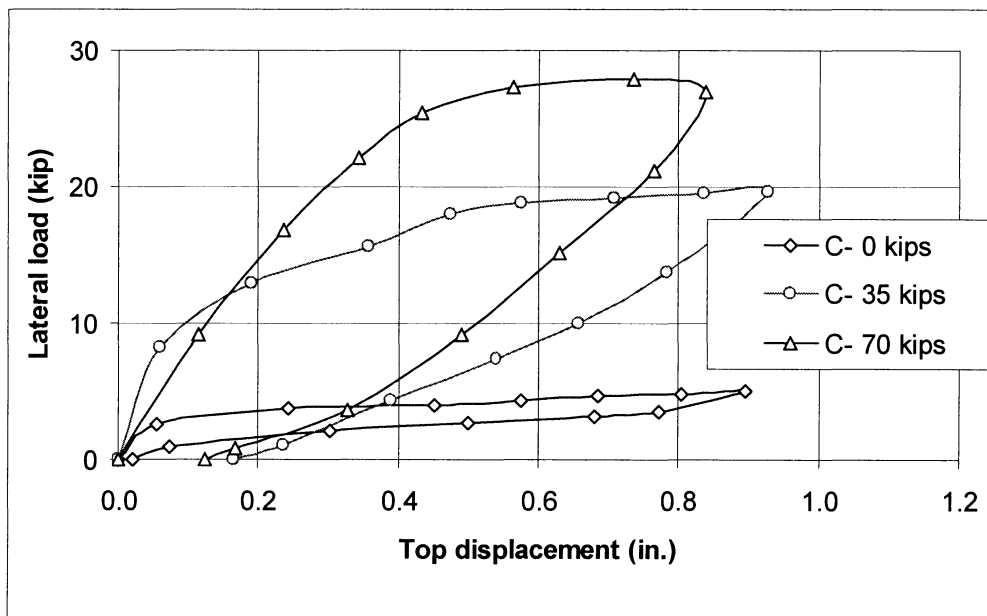


Figure 26. Lateral load/displacement relations of Specimen C

Bending strains of the dowels were recorded during static loading of Specimen C under various vertical loads and presented in Figure 27. Strains were averaged from all channels and were plotted against the relative lateral displacement of the top of the abutment. As seen in the figure, the strain/displacement relationship was approximately linear. The maximum strain measured during the tests was about 50 % of the yield strain of the dowels. The yield strain of the dowels was slightly over 1,400  $\mu\epsilon$ . Bending strains of the test when the vertical load was 70 kips were about 10% higher than the other two tests.

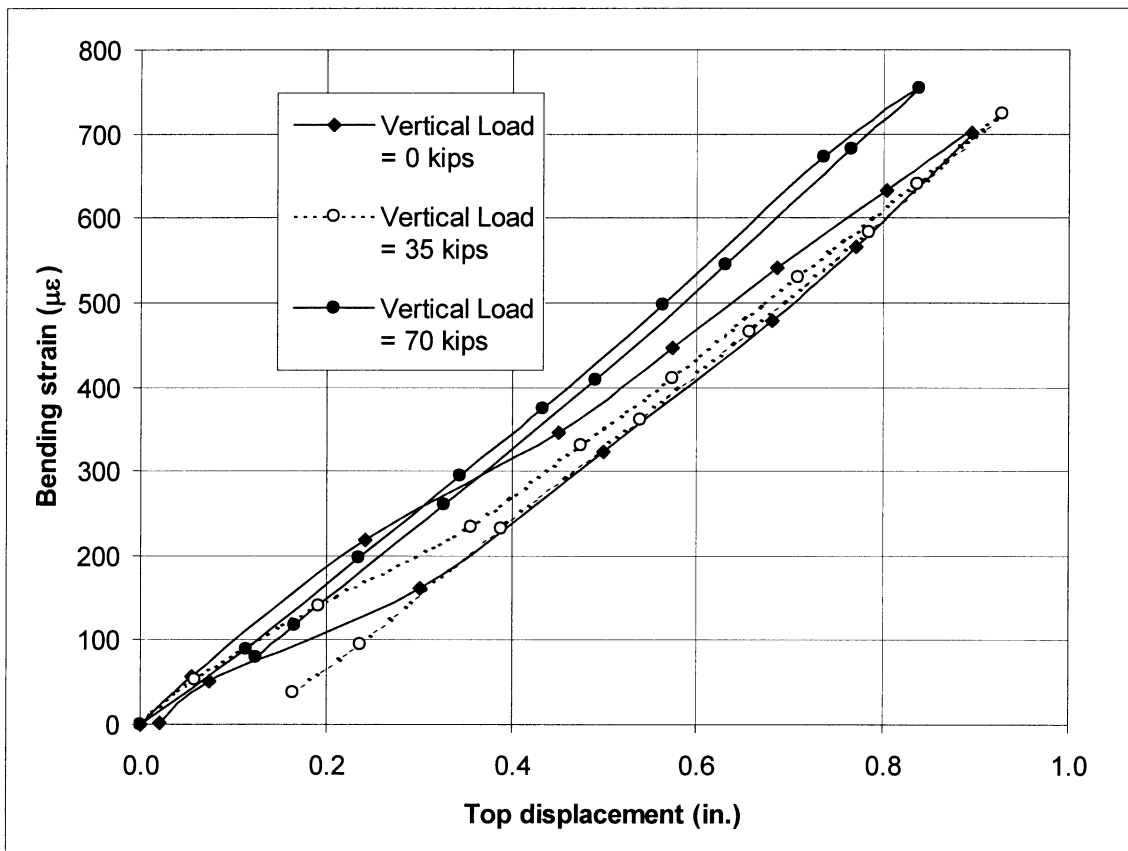


Figure 27. Bending strains measured on dowels of Specimen C

The rotational stiffness of the specimens was calculated as the ratio of the moment around the point of rotation to the rotation of the abutment. Variations of the rotational stiffness as a function of the relative displacement at the top of the abutment are presented in Figure 28 for Specimen C.

### Cyclic Load Tests

Cyclic load tests were carried out following the static load tests on Specimens B and C. Each specimen was tested under 0 and 35 kip vertical loads. Tests were conducted as displacement controlled according to Table 3. Data were collected at the beginning of the test, after the 10<sup>th</sup> year, the 50<sup>th</sup> year, and the 75<sup>th</sup> year of simulated time. Only the data of the first and the last cycles are shown for clarity of the graphs.

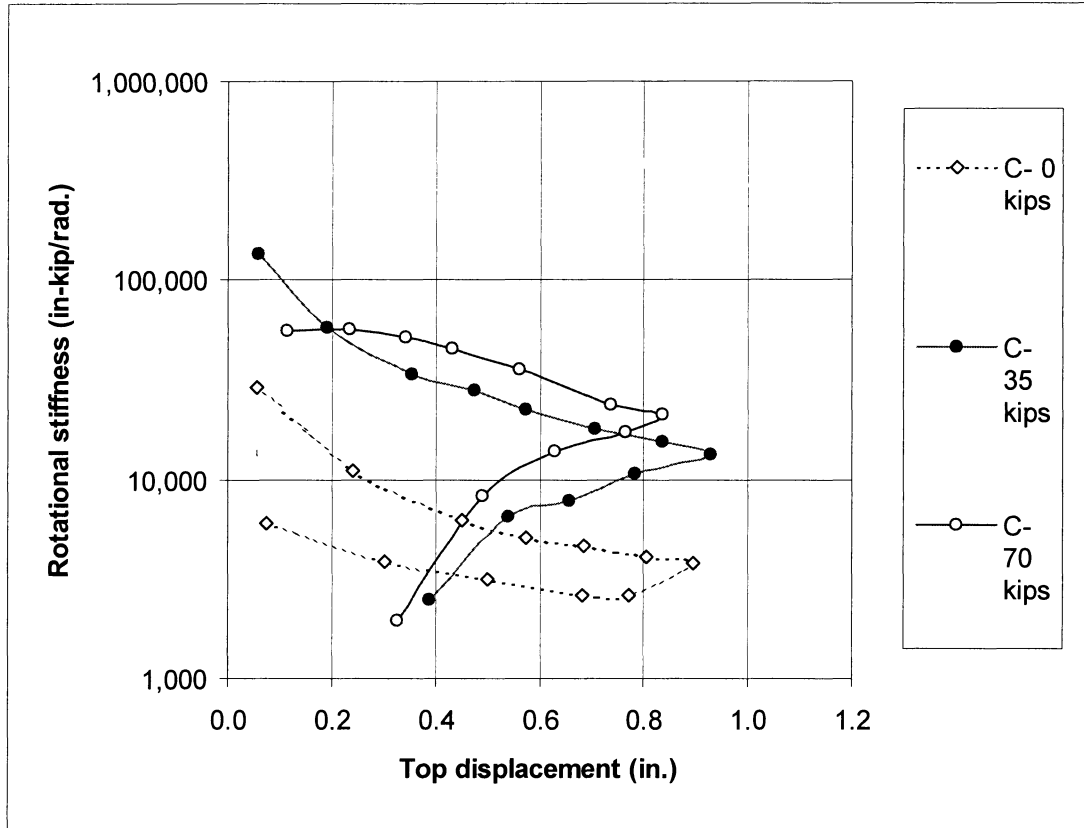


Figure 28. Rotational stiffness of Specimen C during static load tests

Figure 29 shows the lateral load hysteresis loops for Specimen B under 0 vertical load, and Figure 30 shows a similar graph for the same specimen under a vertical load of 35 kips. The latter figure shows half the loops of the data because the data on the other half were unreliable as they were affected by a computer hard drive problem. As seen in these figures, almost no damage was introduced by over 27,000 cycles. Figure 29 indicates no damage, and Figure 30 indicates some softening in load response for 35-kip vertical loading.

Lateral load hysteresis loops for Specimen C under 0- and 35-kip vertical loads are shown in Figures 31 and 32, respectively. As evident in both figures, there is no sign of damage. The load/displacement behavior of the specimen was virtually unchanged after 75 years of displacement cycles. Bending strains of the dowels also showed no change in response to cyclic loading as depicted in Figure 33 for 35-kip vertical loading.

Specimen C was also subjected to 150 cycles consisting of  $\pm 2.5$ -inch displacement cycles at the top of the abutment after the completion of the previous cyclic test program in an attempt to fail the dowels. The lateral load and the bending strain responses of the specimen are presented in Figures 34 and 35, respectively. No vertical load was applied to the specimen. Only the responses of the first and the 150<sup>th</sup> cycles are shown in these figures. Even at these higher rotations, the specimen was able to handle the loads with no sign of damage. The maximum bending strain seen in Figure 35 is slightly higher than the yield strain ( $\sim 1,400\mu\epsilon$ ) of the dowels.

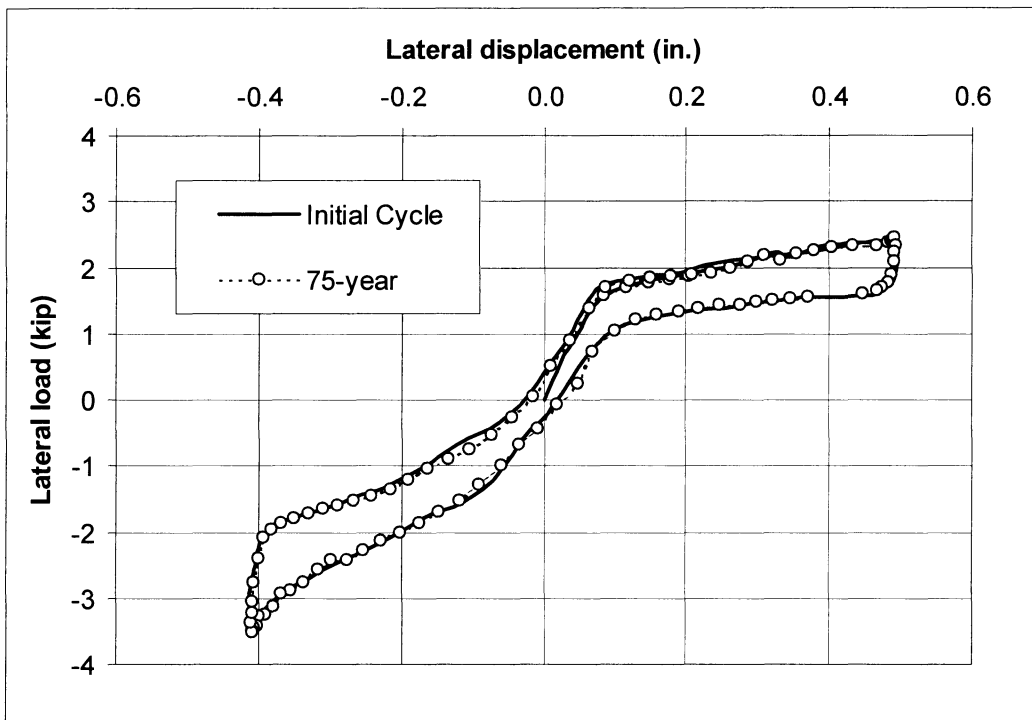


Figure 29. Lateral load/displacement relationship of Specimen B for 0 vertical load

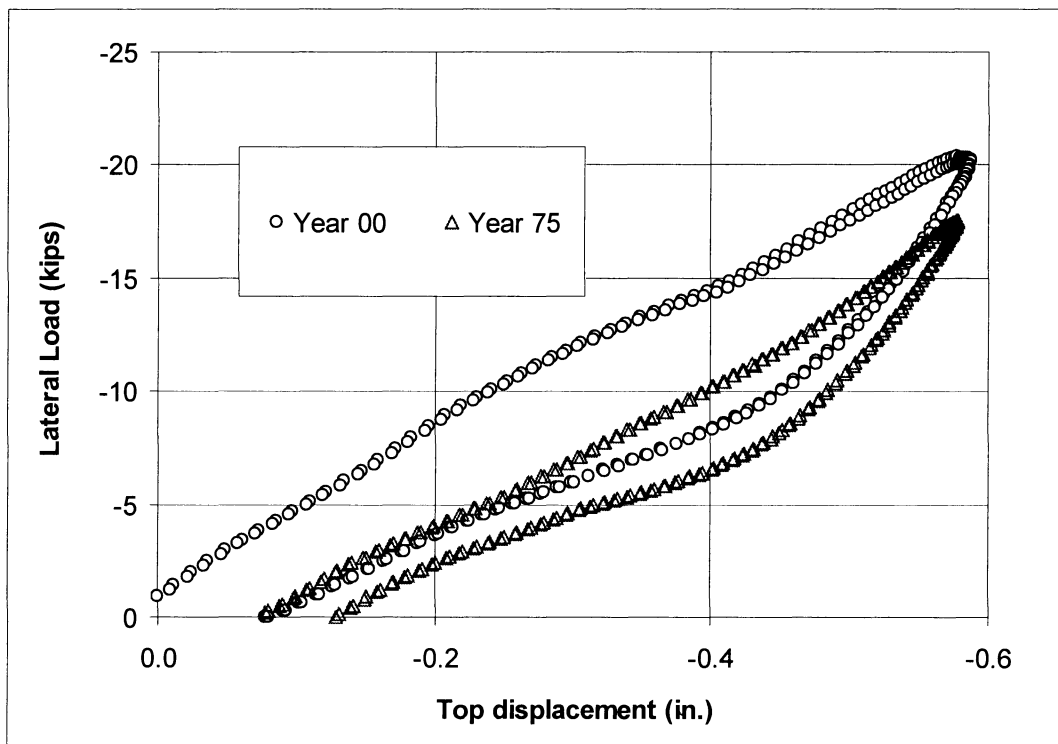


Figure 30. Lateral load/displacement relationship of Specimen B for 35 kip vertical load

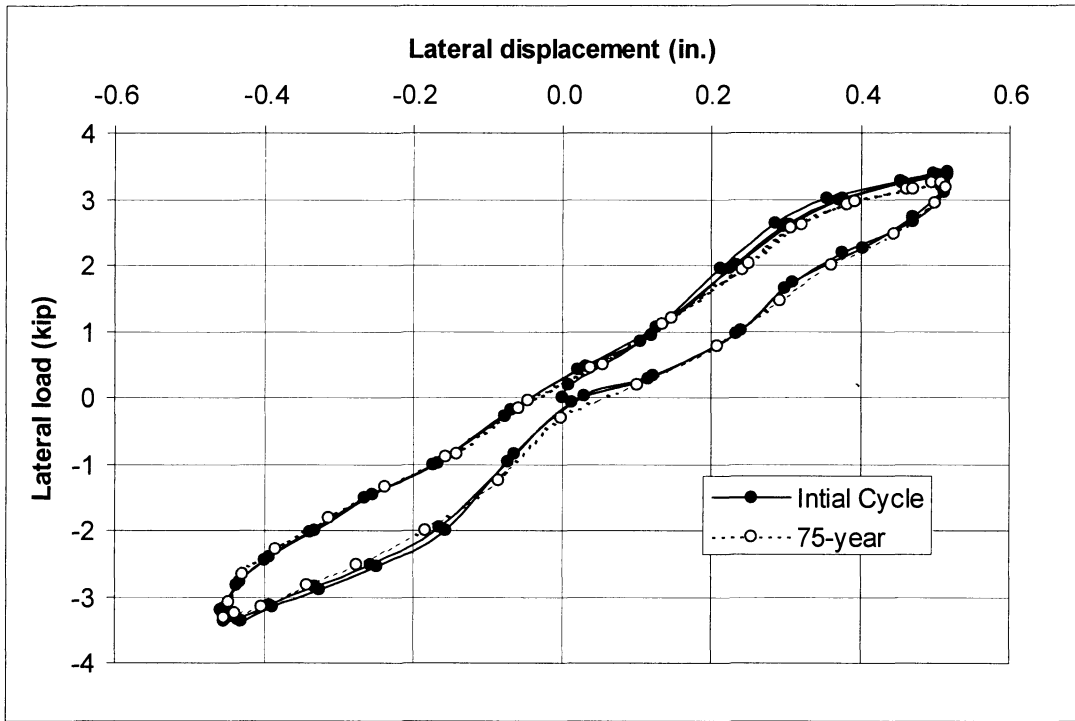


Figure 31. Lateral load/displacement relationship of Specimen C for 0 vertical load

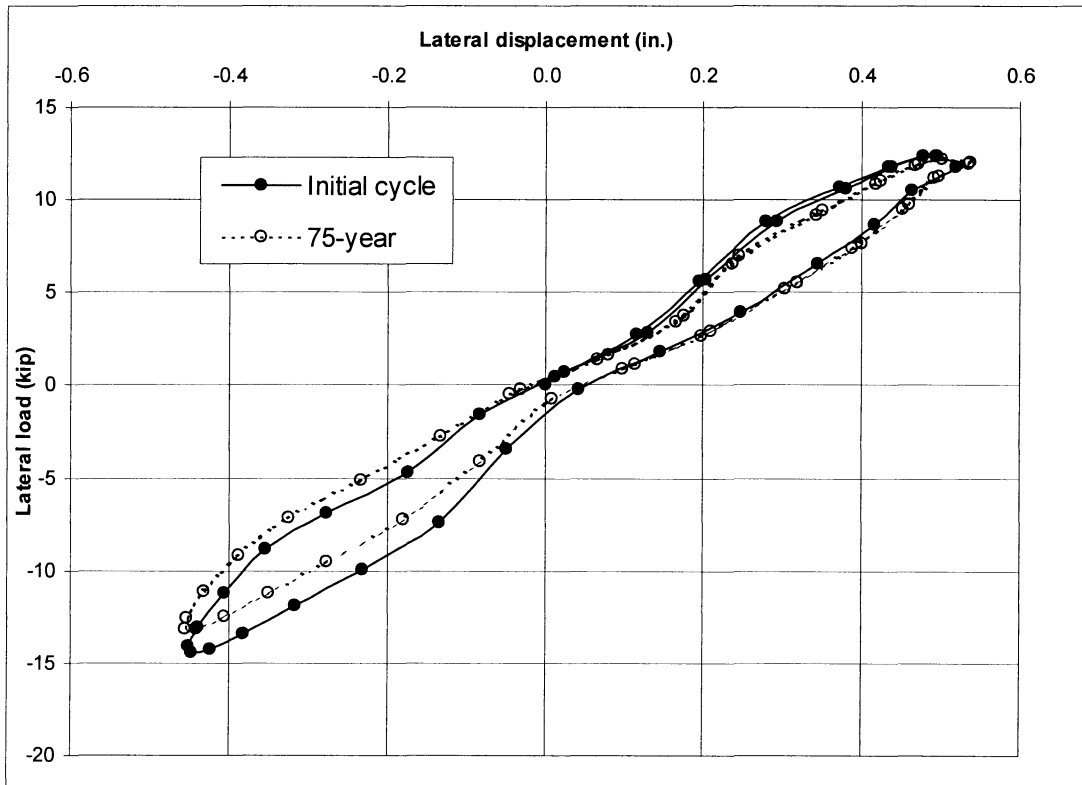


Figure 32. Lateral load/displacement relationship of Specimen C for 35 kip vertical load

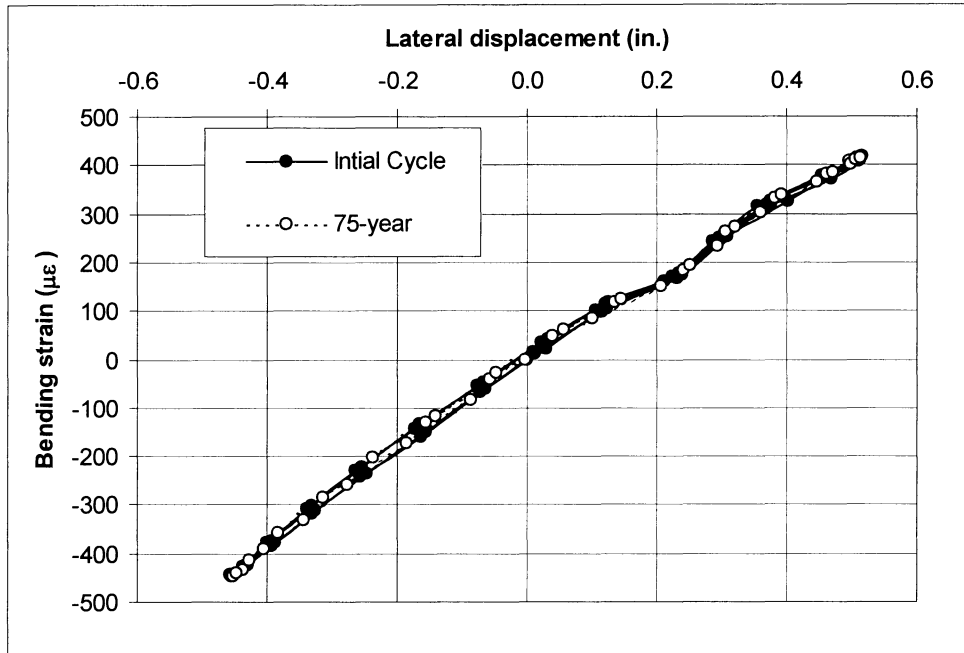


Figure 33. Bending strain/displacement relationship of Specimen C for 35 kip vertical load

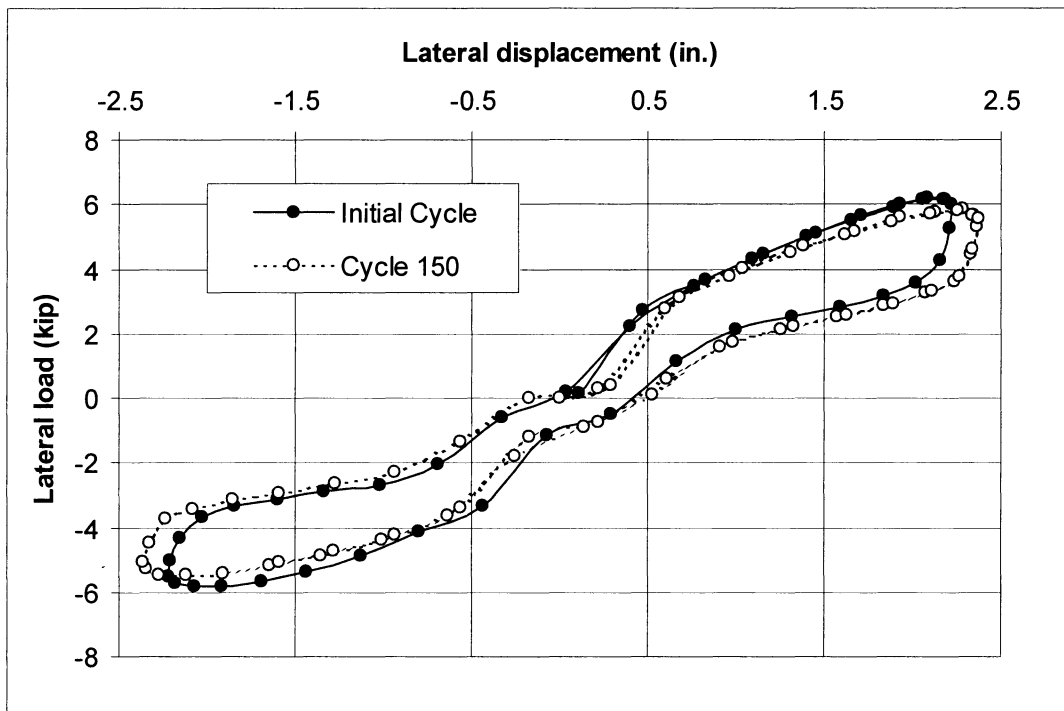


Figure 34. Lateral load/displacement relationship of Specimen C for 0 vertical load during large displacement cyclic tests

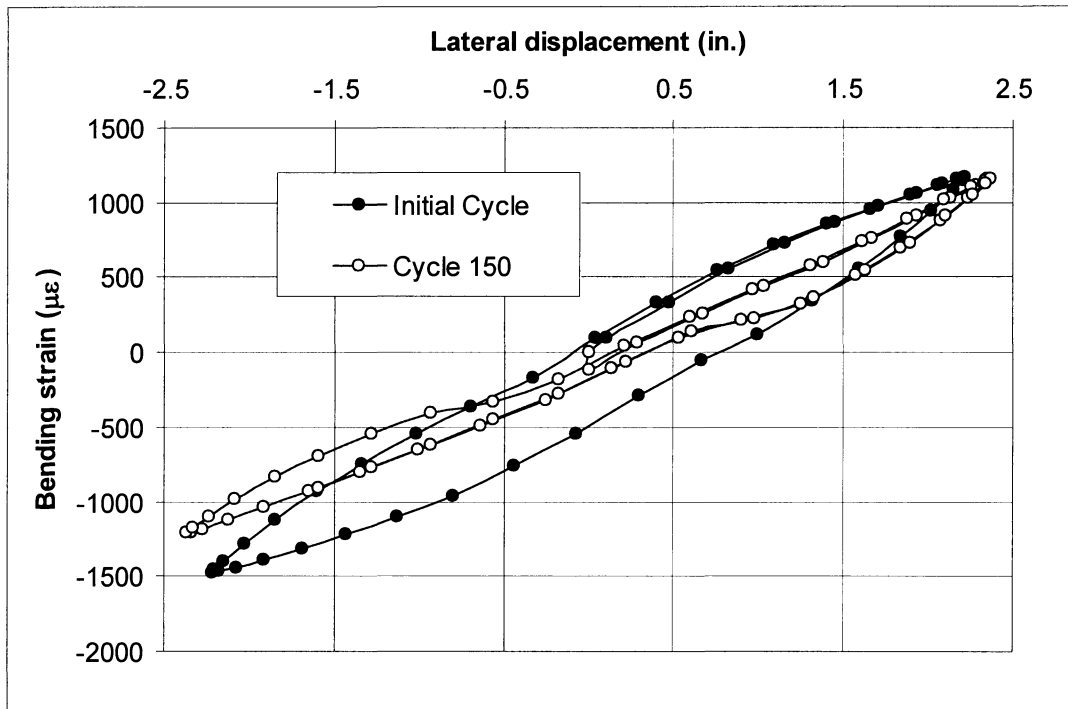


Figure 35. Bending strain/displacement relationship of Specimen C for 0 vertical load during large displacement cyclic tests

## Pile Experiments

### H-pile Tests

Maximum displacement of the pile, measured 53 inches above the pile cap, and the measured strain are summarized in Table 15. In HP-AA and HP-CC series, data were collected during the cycles representing 1, 10, 50, and 75 years. In series HP-BB, 75 years of bridge life were simulated. Data were collected similar to the other series for the simulated years of 1, 10, 50, and 75.

Table 15. Maximum measured displacement and strain in H-pile

Test series	Maximum displacement (in.)	Bending strain ( $\mu\epsilon$ )	Vertical load (kips)	Strain imposed by vertical load ( $\mu\epsilon$ )
HP-AA	0.5	580	38	87
HP-BB	0.5	580	38	87
HP-CC	0.5	580	38	87
HP-DD	0.85	1140	38	87

Figure 36 shows the relationship between the displacement and the lateral load for the HP-BB series. The first and the 75<sup>th</sup> cycle are shown. Displacement and lateral load data were measured 53 and 86 inches above the pile cap, respectively. The maximum bending strain on the pile was about 580  $\mu\epsilon$ . An additional strain of 87  $\mu\epsilon$  (3 ksi compression stress) was also applied to the pile by the vertical loading rams. A comparison between the first (BB-00) and last (BB-75) cycles indicates a slight reduction, about 5%, in the lateral load for a given displacement.

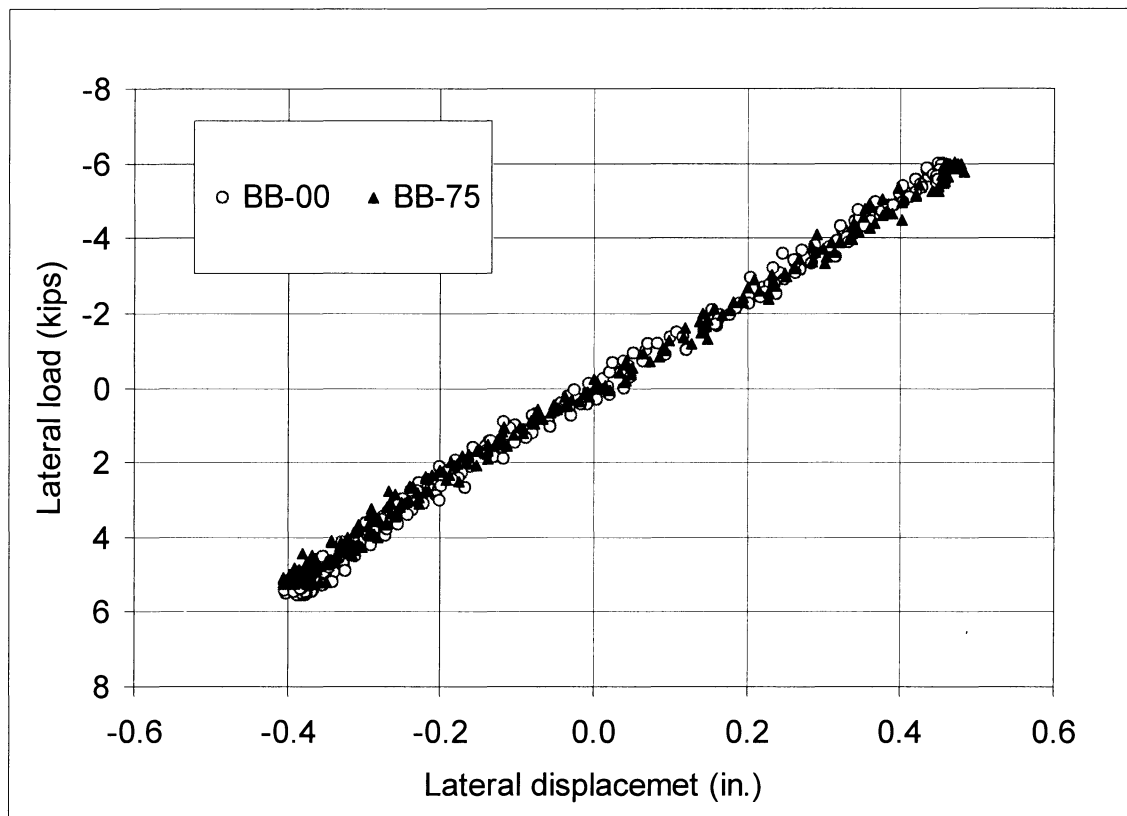


Figure 36. Lateral load vs. displacement relationship in HP-BB series

The HP-DD series was a static load test. A maximum of 1140  $\mu\epsilon$  bending strain was applied in addition to the 87  $\mu\epsilon$  strain (3 ksi compression stress) from the vertical load. As seen in Figure 37, the pile sustained this load without losing its linear load displacement response. A strain of about 1200  $\mu\epsilon$  corresponds to the nominal yield stress of 36 ksi. Observations of the pile and the pile cap yielded no sign of distress.

For a given load, it was found that the maximum measured strain was about half of the strain calculated for a fixed-end column. This can be explained by the fact that the pile was actually not 100% fixed at the pile/pile cap interface. Pile displacements were measured along the pile and are shown in Figure 38 for selected lateral loads. The figure indicates that the slope at the bottom of the pile is not 0, which indicates that the pile behaves as a partially fixed column.

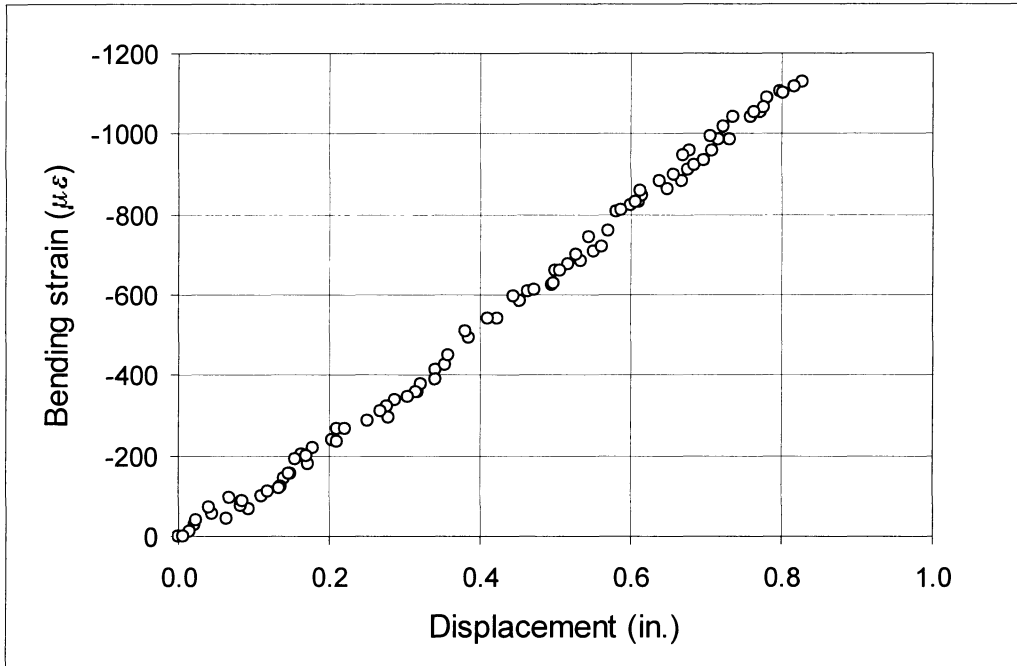


Figure 37. Bending strain vs. displacement relationship in HP-DD series

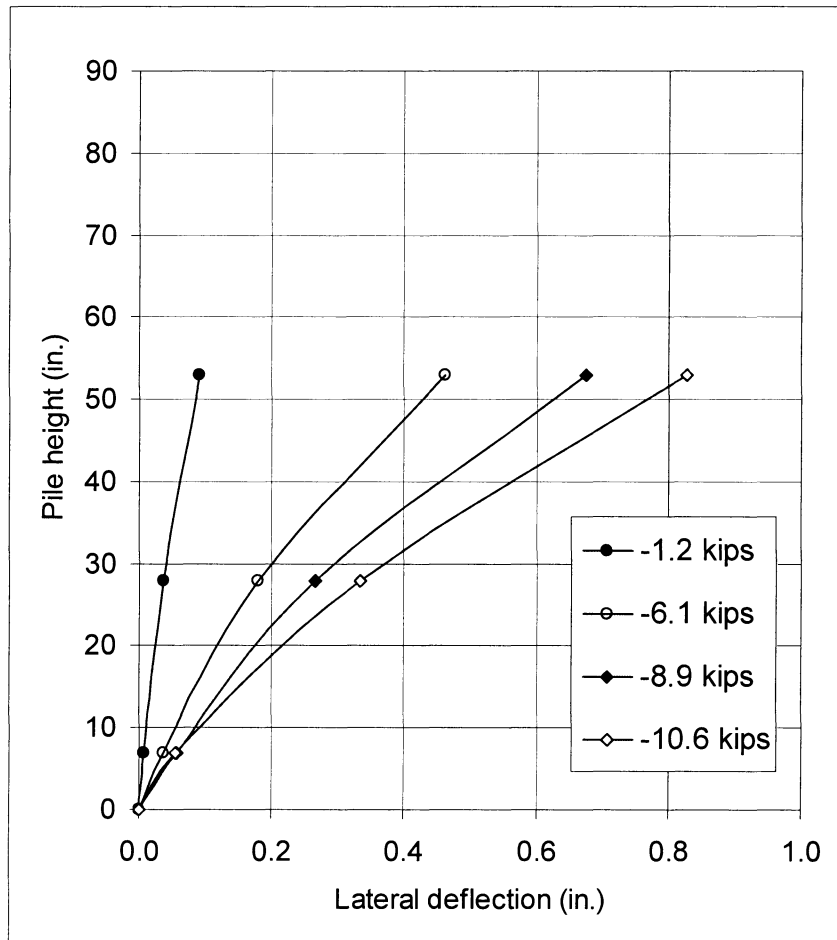


Figure 38. Displacements along the H-pile for selected lateral loads

## Pipe Pile Tests

The stiffness of the pipe pile was almost twice the stiffness of its cap. This and the limited rotational capacity of the steel elements used for mounting the cap onto the reaction floor caused the pile cap to rotate more than the H-piles. When the pile cap rotates, stresses build up around the edges of the pile cap. These higher stresses caused the concrete in this region to chip off during initial trials. Figure 39 shows two pictures of minor damage in pile caps. The top picture shows the debris of the cracked concrete after the cap was removed and shows where the damage was concentrated. The lower picture shows a side view of the pile cap after the test was completed.

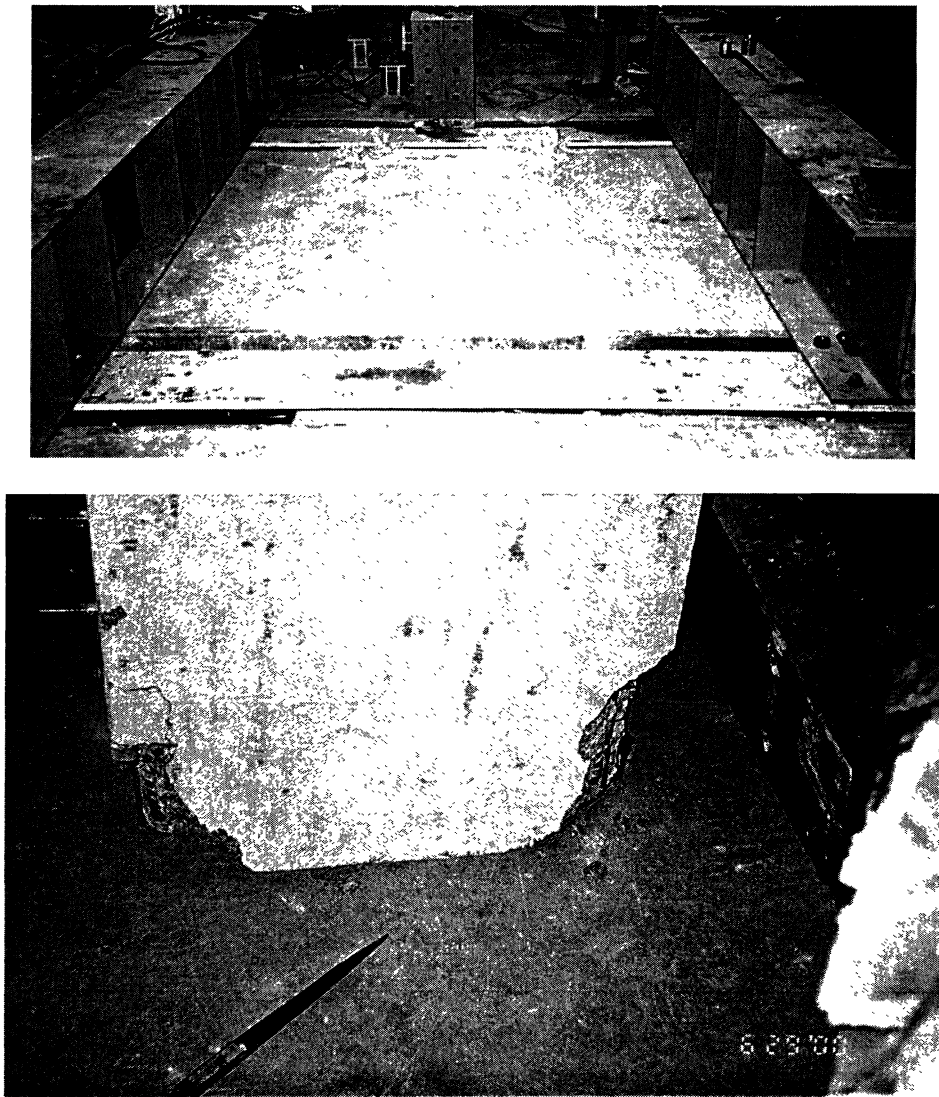


Figure 39. Pictures of damage observed in pile cap during testing

A constant vertical load could not be maintained on the pile. The stresses from the vertical load would have been 2 ksi, which is not significant. Therefore, it was decided to omit the application of the vertical load. Approximately 2,300 cyclic lateral loads were applied to the pile 86 inches above the pile cap. These cycles generated a maximum bending stress of about 4 ksi in the pile. Figure 40 shows the lateral load displacement response of the pile for the first and 2,300<sup>th</sup> cycles. Lateral displacement and lateral loads were measured 53 and 86 in above the pile cap, respectively.

### Prestressed Concrete Pile Tests

Data were collected at the beginning of each test series and at selected intervals. In CP-AA and CP-CC series, data were collected during the cycles of 1, 10, 50, 75, and 150. In series CP-BB, 75 years of bridge life were simulated. Each year was simulated by a combination of small cycles and a large cycle as shown in Table 10. Data were collected in a manner similar to that used in the other series for the years of 1, 10, 50, and 75.

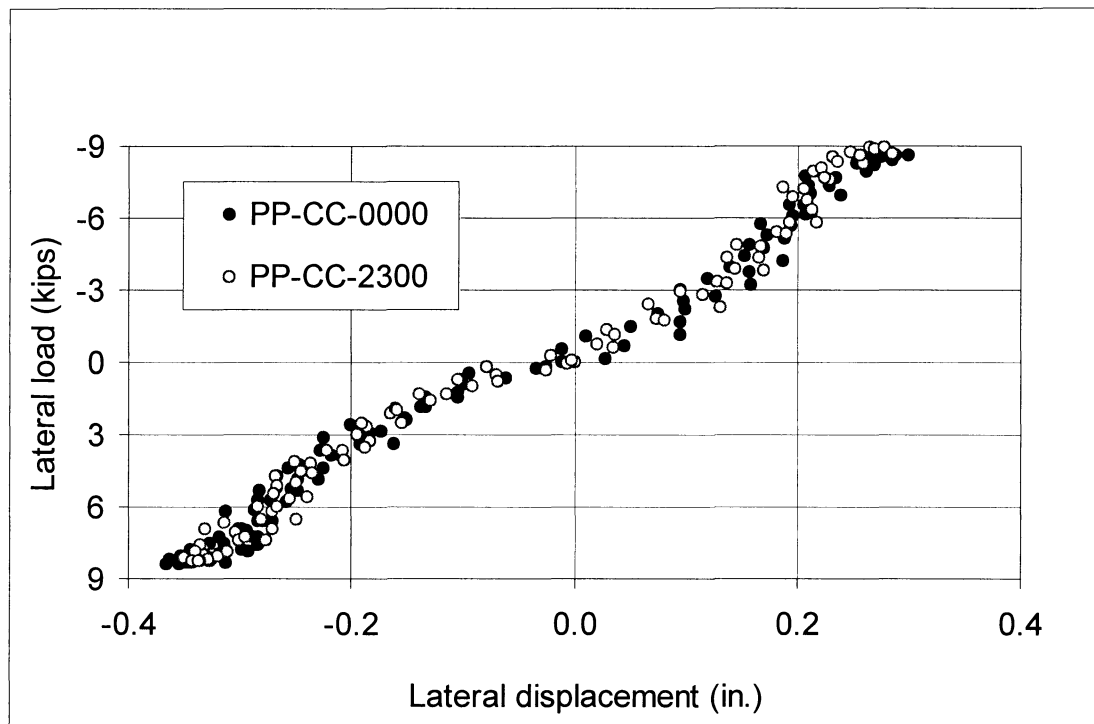


Figure 40. Lateral load vs. displacement relationship in pipe pile test

The concrete in a reinforced concrete element initially carried tension stresses. As soon as the tension capacity of the concrete was reached, the concrete cracked. In order to detect the tension capacity of the concrete, data were recorded in the initial trial cycles. In the first trial cycle, tension cracks at the bottom of the pile developed. One of the cracks passed through one of the strain gages and left it useless. Data obtained from this strain gage until its failure are presented in Figure 41. Displacement values are measured 53 inches above the pile cap. The

other strain gage was operable during the testing period. A picture of the tension crack developed in the pile is shown in Figure 42.

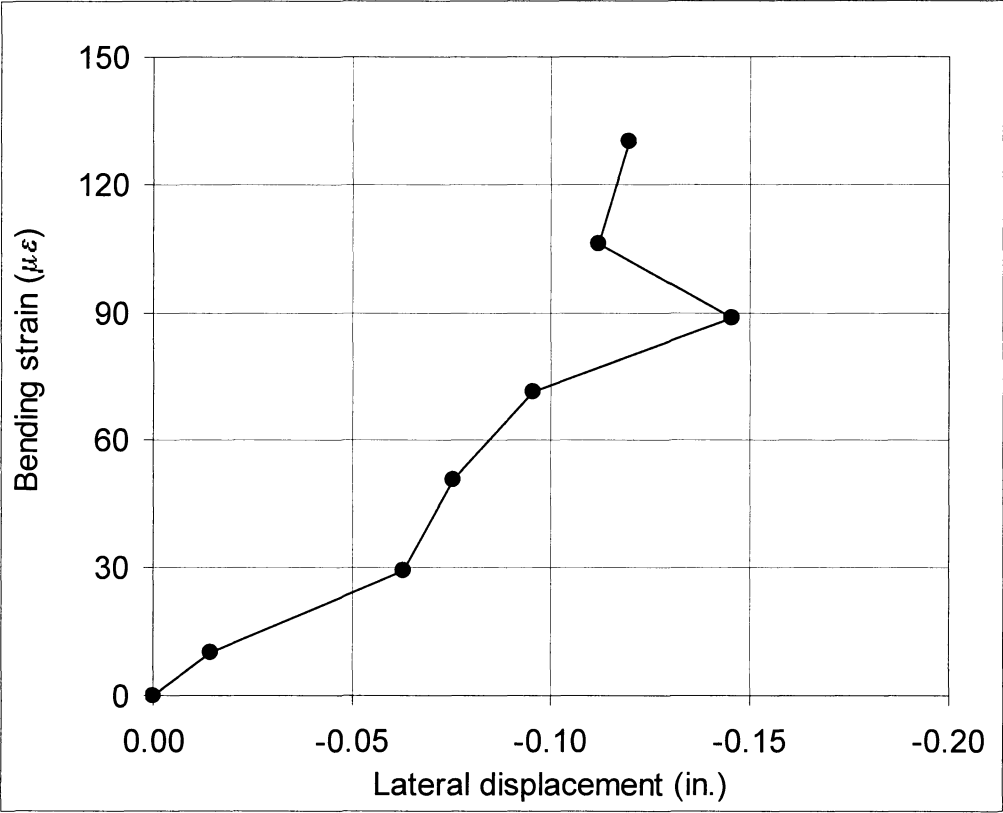


Figure 41. Failure of strain gage because of tension cracks in prestressed concrete pile

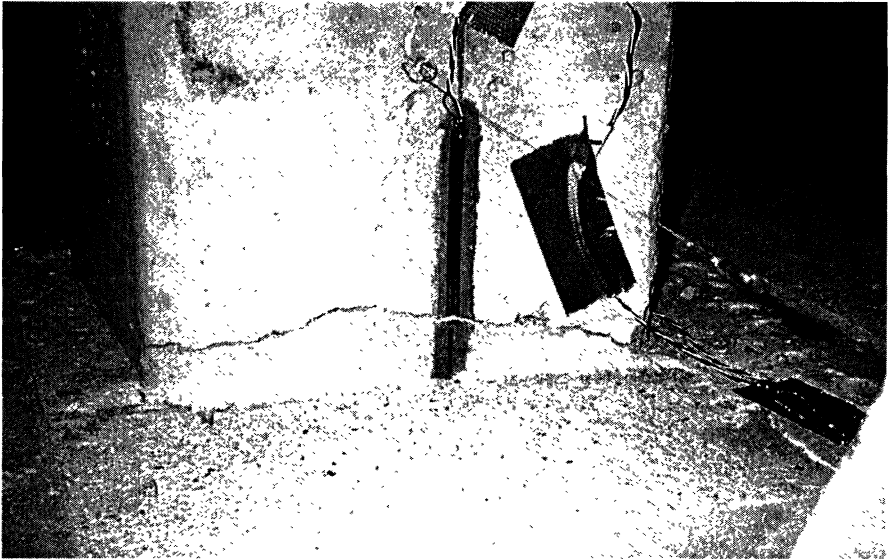


Figure 42. Picture of tension crack developed in prestressed concrete pile in first load cycle

Figure 43 shows the relationship between the displacement and the lateral load for the CP-AA series. In the figure, the first, 10<sup>th</sup>, 50<sup>th</sup>, and 150<sup>th</sup> cycles are shown. Displacement and lateral load data were measured 53 and 86 inches above the pile cap, respectively. For a given displacement, the figure indicates continuous reductions in the bending stresses with increasing cycles.

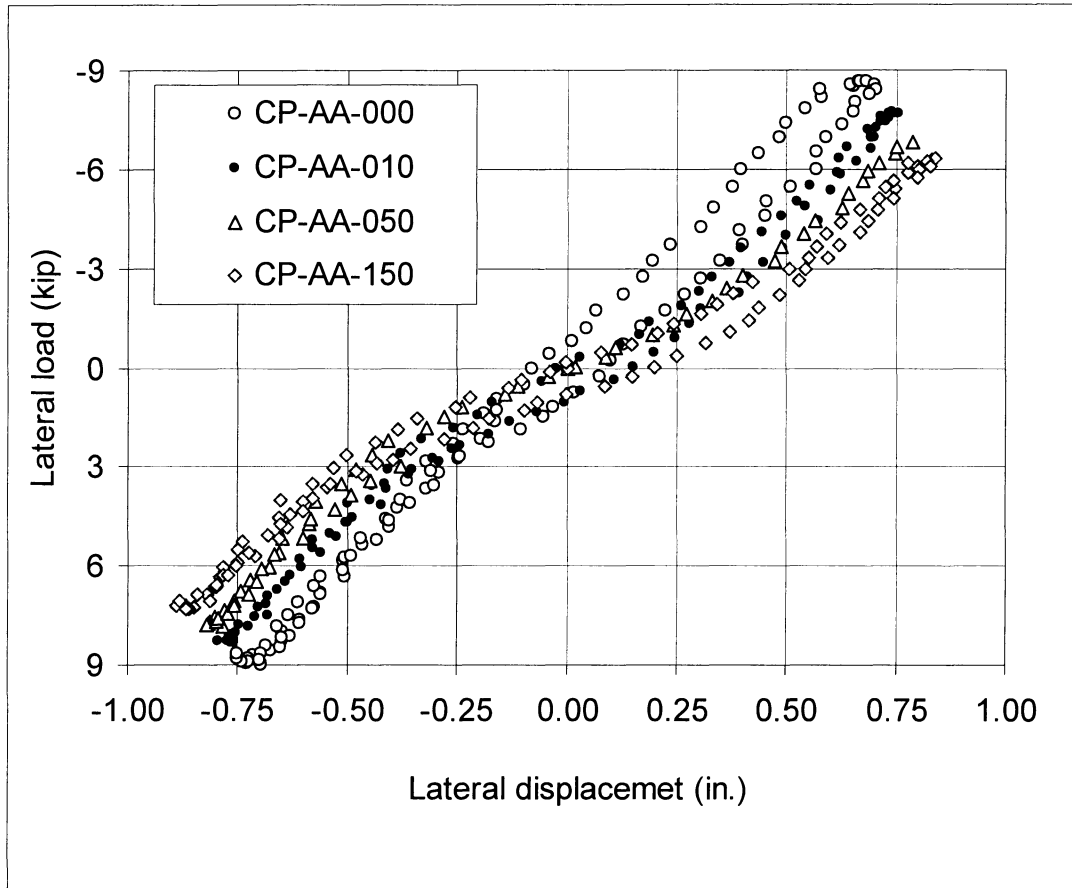


Figure 43. Lateral load vs. displacement relationship in CP-AA series

It was observed during testing that tension cracks developed progressively in the pile starting from the bottom of the pile to the top of the pile. The distance between the two adjacent cracks varied between 7 and 11 inches. A total of five tension cracks were visible. The first one was about 2 inches above the pile cap, and the last tension crack was about 40 inches above the pile cap. The tension cracks gradually enlarged as the load cycles continued.

The reduction in lateral load for a given lateral displacement continued to take place in the CP-BB series. This appeared to be associated with the progressive deterioration caused by the tension cracks. In the CP-CC series, no further reduction in lateral load occurred. It is clear from the load displacement behavior that the damage in the concrete pile was more pronounced in the early cycles. It also appears that larger cycles create most of the damage.

## Soil-Structure Interaction Effects

The loads applied laterally in the finite element analyses represent the forces exerted on the abutment by the superstructure (the girders and the deck) as the temperature increases or decreases and the superstructure expands or contracts. The stiff girders and the attached deck tend to restrain rotation of the abutment, and the flexural stiffness ( $EI$ ) of the superstructure is included in the analyses models. However, the axial stiffness ( $EA$ ) of the girders and the bridge deck are set equal (approximately) to 0, so that the applied load will be proportional to the desired lateral displacement. The lateral forces were applied to the abutment along the neutral axis of the bridge girders.

The characteristics of the finite element model and results are thus:

- The applied force corresponds to the lateral forces exerted on the abutment by the superstructure as temperatures increase or decrease.
- The resulting displacements and rotations of the abutment correspond to the actual displacements and rotations due to temperature increase and decrease.
- The forces induced in the abutment, the approach fill, the foundation piles, and the foundation soils show how the loads are carried by increased earth pressures in the approach fill and increased shear forces on the foundation piles.

### Effects of Approach Fill

The effects of the approach fill on pile stresses were studied by conducting two sets of finite element analyses. The first set of analyses investigated the pile stresses with no approach fill. The second set of analyses investigated the pile stresses with an approach fill. Lateral forces were applied through the bridge beams such that the displacement at the pile head was the same for both sets of analyses. Any difference in the pile stresses was thus due to the approach fill.

The results of these analyses indicated that the approach fill significantly reduces the pile stresses. This beneficial reduction in the stresses occurs because the approach fill drags the foundation soil as it moves, resulting in less resistance of the foundation soil against the pile displacements. In other words, the foundation soil acts as if it were softer when the approach fill is in place. It would therefore be excessively conservative to perform analyses of the lateral loads on the foundation piles without recognizing this effect.

Reductions in the maximum shear due to approach fill were calculated for three sand densities and are tabulated in Table 16. Reductions in shear were significant, ranging from 40% for loose sand to 64% for dense sand. The computed values of slope at the pile head are also shown in this table. It can be seen that the slope of the pile head increases as the foundation soil gets more dense. This occurs because the dense sand offers greater resistance to lateral displacement of the piles, and more pile head rotation is required to achieve the same pile head displacement.

Additional finite element analyses were conducted to compare the effects of bridge expansion and contraction on pile stresses. Lateral forces were applied to pull the abutment away from the approach fill, such that the pile head displaced about 0.68 inch. The foundation soil was assigned the properties of medium dense sand.

These analyses indicated a slightly smaller beneficial effect of the approach fill for the case where the bridge contracted. The reduction in the shear due to the presence of approach fill was 47% in this case, as compared to 51% in the case of expansion. The stresses in the pile were found to be about 5% higher for 0.68-inch movement of pile head away from the approach fill than for 0.68-inch movement of pile head towards the approach fill.

Table 16. Reductions in maximum pile stresses due to approach fill

Foundation Soil	Displacement at pile head (in.)	Slope at pile head** (rad.)	Reduction in Shear*
Dense Sand	0.70	0.0065	64%
Medium Dense Sand	0.68	0.0056	51%
Loose Sand	0.70	0.0054	40%
* As compared to the analyses with no approach fill			
** For cases with approach fill.			

### Effects of abutment type: full integral vs. integral with hinge

Finite element analyses were conducted to compare the behavior of full integral and integral with hinge abutments. The foundation soil was assigned the properties of medium dense sand. Loads were applied through the bridge beams to induce 2 inches of displacement toward the approach fill in both cases.

Figure 44 shows the displaced positions of the full integral and the integral with hinge abutments in medium dense sand. As can be seen in this figure, the bottom of the integral abutment with hinge rotates more than the top, which is restrained by the bridge beams. The shear force in the dowels and the interactions among the pile cap, the soil, and the piles controls the rotation of the lower portion of the integral abutment with hinge.

The larger slope at the tops of the piles under the integral abutment with hinge is beneficial to the pile stresses. In addition, it can be seen in Figure 44 that piles supporting the integral abutment with hinge displace less than those supporting the full integral abutments. As a result of these effects, the computed pile stresses were about 10% lower for the integral abutment with hinge.

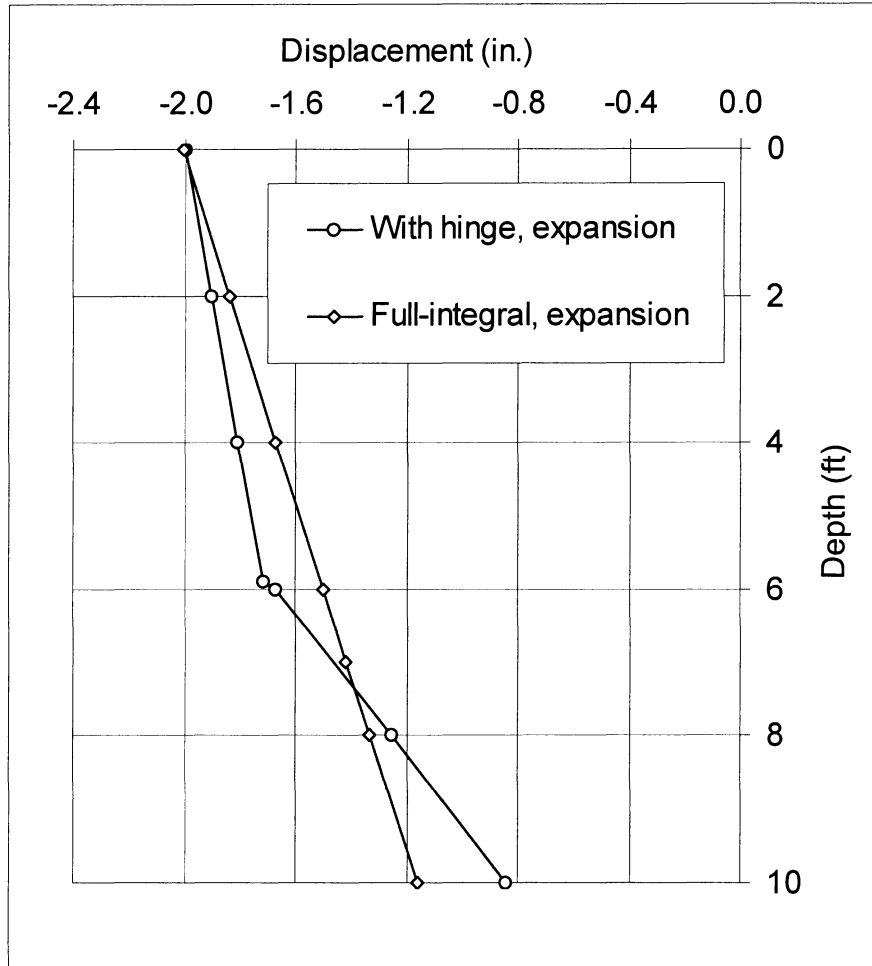


Figure 44. Displacement behaviors of full integral and integral with hinge abutments in expansion mode of bridge in medium dense sand

The behavior of the integral abutment with hinge was also explored in the contraction mode of the bridge by applying a lateral load through the bridge beams to pull the abutments away from the approach fill. An integral abutment with hinge and a full integral abutment were pulled such that the tops of the abutments displaced 2 inches toward the bridge centerline. Figure 45 shows the displaced position of both abutments in medium dense sand. It can be seen that the bottom of the integral abutment with hinge rotates more than the top and that the displacement at the top of the piles is less than for the full integral abutment, as was the case in the expansion mode. The computed pile stresses were 40% smaller for the integral abutment with hinge than for the full integral abutment.

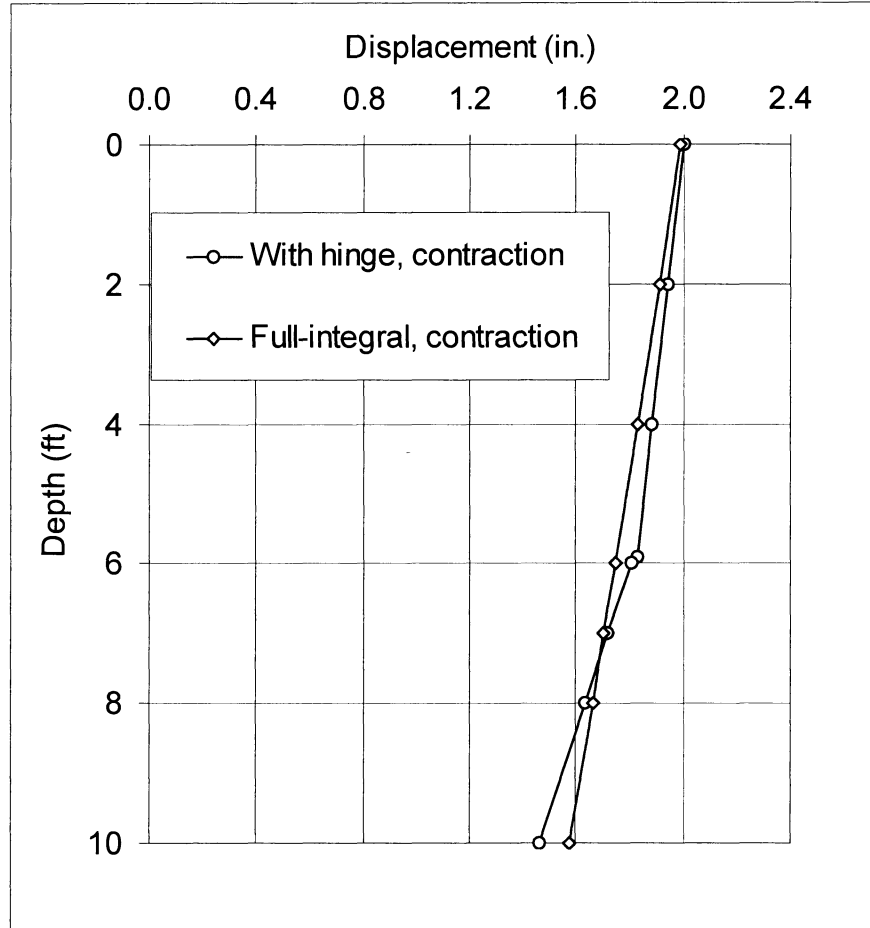


Figure 45. Displacement behaviors of full integral and integral with hinge abutments in contraction mode of bridge in medium dense sand

## DISCUSSION

### Steel H-pile

The H-pile subjected to weak axis loading exhibited the best behavior among the piles tested. The pile sustained stresses in excess of 20 ksi in cyclic loading and 35 ksi in static loading without any sign of distress. Based on this performance, the H-pile would survive temperature-induced cyclic loads up to its nominal rated yield stress of 36 ksi. Coupled with the test results, the ease of availability of the H-piles makes it the best choice for support of integral bridges.

### Pipe pile

A 14-inch steel pipe pile with a 5-inch wall thickness has a stiffness that is significantly larger than that of the H-pile tested. An abutment supported by this type of pile would be subject

to stresses that are much higher than an abutment supported on H-piles with weak axis orientation. However, there is some evidence that the abutment would be the first to fail if either one were to fail. This is because, for a given displacement, stiffer piles are subjected to higher lateral loads.

### **Prestressed Reinforced Concrete Pile**

Test results for the concrete pile did not reflect the effect of the vertical load, which would be expected to be detrimental. It is anticipated that the damage in the prestressed concrete pile would have been even more severe if a vertical load had been maintained on the pile. As the pile was pushed laterally, the concrete area available to resist the compression stresses from the vertical load became smaller because of the tension cracks that had developed. At the end of the tests, it was observed that the contact area had dropped below 20% of the original cross-sectional area of the pile. Under this condition, the compressive stress induced by the vertical load would be considerably increased. Therefore, it appears that the use of concrete piles to support integral abutment bridges is not the best choice, because of the possibility that they might crack and undergo cumulative damage under cyclic loading.

### **Proposed Method to Account for Soil Structure Interaction Effects in Design of Piles Supporting Integral Abutment Bridges**

Finite element analyses indicated that movements of the approach fill cause the foundation soil to behave as if it were softer. This is somewhat analogous to soil-pile-soil interaction in pile groups. As a result of this interaction, piles in a group carry smaller shear loads and are less severely stressed than are single piles subjected to the same displacement at the pile head. A conventional way of considering the pile group effects is to reduce the soil resistance using p-multipliers. A similar procedure can be used in the case of piles supporting integral bridges as a means of accounting for approach fill/foundation soil interaction.

The p-multiplier concept can be used to allow for the beneficial approach fill effect when computer programs such as LPILE are used for analysis and design of piles for integral bridges. Appropriate values of p-multiplier range from about 0.1 for stiff soil conditions to about 0.5 for soft soil conditions. If refinement of these factors appears warranted, 2D finite element analyses of the type described here could be used in conjunction with LPILE analyses.

The following is a step-by-step procedure that can be used to design the piles of integral bridges using computer programs such as LPILE:

Step 1: Estimate the maximum displacement at the top of the pile head.

Step 2: Estimate the slope at the pile head.

Step 3: Use the p-multiplier values recommended above.

Step 4: Calculate the shear and moment, using a computer program such as LPILE.

## CONCLUSIONS

- The behavior of the revised integral abutment with hinge is superior to the original design, as it showed no sign of damage after applying over 27,000 displacement cycles.
- Integral abutments with hinges may make longer integral bridges possible.
- Integral abutments with hinges can significantly reduce the moments transferred from the superstructure down to the foundation piles.
- Steel H-piles oriented in weak-axis bending are the best pile type for support of integral abutment bridges.
- For a given displacement, shear stresses in an abutment supported by pipe piles will be higher than shear stresses in an abutment supported by steel H-Piles in weak axis bending.
- Seasonal temperature variations are important for concrete piles. The total number of daily temperature cycles is important for the H-pile.
- Stiff piles increase the likelihood of abutment distress. Less stiff piles serve to protect the integrity of the abutment.
- Piles are not fully fixed at the pile/pile cap interface. In the H-pile and pipe pile tests, measured stresses were about half of the theoretical stresses of the fully fixed-head piles.
- Cyclic loading damage to steel piles of integral bridges is not expected as long as the total stress induced in the pile does not exceed the yield strength of the steel.
- The finite element analyses indicate appreciable rotations occur in integral abutments, resulting in the shear and moment reductions in the piles. Interactions between the approach fill and the foundation soil create further favorable conditions with respect to pile stresses because the foundation soil behaves as if it were softer when the movement of the approach fill displaces it.
- The p-multiplier concept can be used to allow for the beneficial approach fill effect when computer programs such as LPILE are used for analysis and design of piles for integral bridges.
- The finite element analyses indicate that integral abutments with hinges offer benefits over full integral abutments.

## RECOMMENDATIONS

1. *Use steel H-piles oriented in weak-axis bending for support of integral abutment bridges.* Stiff pipe piles are not recommended, as the likelihood of abutment distress will increase. Concrete piles are not recommended because under lateral loads, tension cracks progressively worsen and significantly reduce the vertical load carrying capacity of these piles.
2. *If pipe piles and prestressed concrete piles are to be used for integral abutment bridges, use smaller size piles than used in this investigation.* Further, steps must be taken to reduce the lateral stiffness and allow more rotation to take place at the connection to the pile cap.

## RECOMMENDATIONS FOR FUTURE RESEARCH

1. *Instrument abutments of integral bridges and piles supporting integral bridges to investigate the rotation behavior of integral abutments with hinges, and to investigate pile stresses. Data from such tests would be very useful in validating the findings of this study.*
2. *Conduct experiments and analyses to determine the percentage reduction in bending stresses for weak-axis orientation of H-piles compared to strong-axis orientation.*
3. *Expand the LPILE analyses to include a sensitivity study for p-multiplier values, an example problem with input and output values, and an evaluation of the main difficulties in modeling integral pile behavior.*

## ACKNOWLEDGMENTS

This research was prepared for and funded by the Virginia Transportation Research Council (VTRC) and Virginia Department of Transportation (VDOT). Park Thompson from the Staunton District provided informative discussions about the performance and maintenance aspects of the integral bridges in the district. Ed Hoppe from VTRC contributed to the research by giving his time and by discussing various aspects of integral bridge issues. These contributions are gratefully acknowledged. Tom Murray contributed significantly to this research program by reviewing construction plans and recommending solutions to many difficulties encountered. A special thanks goes to T.E. Cousins for his help with the data acquisition system. Contributions of the technicians Dennis Hoffman, Brett Farmer, and Clark Brown are greatly acknowledged. A special note of recognition goes to Virginia Tech graduate students (former and current) Bob Mokwa, Emmet Sumner, Angela Terry, Micheal DeFreese, David Mokarem, Diane Baxter, and Harry Cooke for their assistance at various stages of this project.

## REFERENCES

- Arsoy, S. (2000). *Experimental and analytical investigations of piles and abutments of integral bridges*, Ph.D. Dissertation, Department of Civil Engineering, Virginia Tech, Blacksburg.
- Arsoy, S.; Barker, R. M.; and Duncan, J. M. (1999). *The behavior of integral abutment bridges*. VTRC 00-CR3. Virginia Transportation Research Council, Charlottesville.
- Bentler, D. J.; Morrison, C. S.; Esterhuizen, J. J. B.; and Duncan, J. M. (1999). *SAGE user's guide, Center for Geotechnical Practice and Research*. Department of Civil Engineering, Virginia Tech, Blacksburg.

- Duncan, J. M.; Bryne, P.; Wong, K. S.; and Mabry, P. (1980). *Strength, stress-strain and bulk modulus parameters for finite element analysis of stresses and movements in soil masses*. UCB/GT/80-01. University of California, Berkeley.
- Girton, D. D.; Hawkinson, T.R.; and Greimann, L.F. (1991). Validation of design recommendations for integral-abutment piles. *Journal of Structural Engineering*, Vol. 117, No. 7, July, pp. 2117-2134.
- Hoppe, E. J., and Gomez, J. P. (1996). *Field study of an integral backwall bridge*. VTRC 97-R7. Virginia Transportation Research Council, Charlottesville.
- James, M. L.; Smith, G. M.; Wolford, J. C.; and Whaley, P. W. (1994). *Vibration of mechanical and structural systems*, Second Edition. Harper Collins College Publishers, New York
- Jorgensen, J. L. (1983). *Behavior of abutment piles in an integral abutment in response to bridge movements, bridges and culverts*. Transportation Research Board, No. 903, pp. 72-79.
- Lawver, A.; French, C.; and Shield, C. K. (2000). *Field Performance of an integral abutment bride*. Presentation at the Annual TRB Meeting, Washington, DC.